RISK-BASED MULTI-THREAT DECISION-SUPPORT METHODOLOGY FOR LONG-TERM BRIDGE ASSET MANAGEMENT

VOLUME 1: AI-BASED BRIDGE-LEVEL DECISION SUPPORT

Alireza Ghavidel
THE UNIVERSITY OF TEXAS AT SAN ANTONIO
Ao Du
THE UNIVERSITY OF TEXAS AT SAN ANTONIO
Sabarethinam Kameshwar
LOUISIANA STATE UNIVERSITY

TECHNICAL REPORT DOCUMENTATION PAGE

1. Report No. https://hdl.handle.net/20.500.12588/6980	2. Government Accession No.	3. Recipient's Catalog No.
4. Title and Subtitle Risk-Based Multi-Threat Decision-Support Methodology for Long-Term Bridge Asset Management Volume 1: AI-Based Bridge-Level Decision Support		5. Report Date March 15, 2024 6. Performing Organization Code:
7. Author(s) Alireza Ghavidel (ORCID: 0000-0003-2273-6943) Ao Du (ORCID: 0000-0001-5808-7856) The University of Texas at San Antonio Sabarethinam Kameshwar (ORCID: 0000-0003-0205-8022) Louisiana State University		8. Performing Organization Report No.
9. Performing Organization Name and Address The University of Texas at San Antonio 1 UTSA Circle, San Antonio, TX 78249		10. Work Unit No. 11. Contract or Grant No. 693JJ321C000027
12. Sponsoring Agency Name and Address Office of Bridges and Structures Federal Highway Administration 1200 New Jersey Ave SE Washington, DC 20590		13. Type of Report and Period Volume 1 Report September 2021- December 2023 14. Sponsoring Agency Code
15. Supplementary Notes		

16. Abstract

This project develops a methodology and tools for a risk-based multi-threat decision-support tool for long-term bridge asset management (BAM), with a particular focus on chronic aging-induced condition deterioration, and more abrupt and extreme seismic hazard impact. Specifically, a stochastic bridge condition deterioration and seismic damage simulation module is developed. Bridge condition deterioration is modeled through Markovian state transition dynamics considering different maintenance actions. Seismic fragility modeling and risk assessment is carried out, considering site-specific seismic hazard and the effect of seismic retrofitting actions. A life cycle cost analysis module is introduced to holistically quantify and aggregate the direct and indirect costs incurred from bridge condition deterioration, seismic damage, and intervention actions over a planning horizon. Benefit-cost analysis for various seismic retrofitting actions is also performed. Finally, by integrating the above bridge deterioration and seismic damage simulation module and the life-cycle cost analysis module with the advanced AI technique, deep reinforcement learning (DRL), a methodology for generating AI-based policies for sequential maintenance decision support for a portfolio of bridges is proposed. Departing from traditional condition-based decision policies, these AI-based policies can offer much more proactive and adaptive decisions to minimize the long-term life-cycle costs. Owing to the parametrized DRL formulation, the AI-based policies can flexibly accommodate the decision needs from different individual bridges within a bridge portfolio in near real time. Practical action constraints are also introduced to align with real-world engineering practices. The proposed AI-based policies are evaluated based on individual bridges as well as on a portfolio of bridges, and demonstrate superior performance in reducing the life-cycle costs compared with other condition-based policies. In addition, the AI-based policies also exhibit robustness to potential human override. Finally, effect of seismic retrofitting, when coupled with AI-based agents, is evaluated for more comprehensive life-cycle benefit-cost evaluation of seismic retrofit actions.

17. Key Words Bridge asset management, Markovian transition matrix, Seismic fragility and risk modeling, Life-cycle analysis, Artificial intelligence		18. Distribution Statement No restrictions.	
19. Security Classif. (of this report) Unclassified	20. Security Classif. (of this page) Unclassified	21. No. of Pages 74	22. Price

Form DOT F 1700.7 (8-72) Reproduction of completed page authorized.

SI* (MODERN METRIC) CONVERSION FACTORS

APPROXIMATE CONVERSIONS TO SI UNITS

Symbol	When You Know	Multiply By	To Find	Symbol
		LENGTH		
in	inches	25.4	millimeters	mm
ft	feet	0.305	meters	m
yd	yards	0.914	meters	m
mi	miles	1.61	kilometers	km
		AREA		
in^2	square inches	645.2	square millimeters	mm^2
ft^2	square feet	0.093	square meters	m^2
yd^2	square yard	0.836	square meters	m^2
ac	acres	0.405	hectares	ha
mi^2	square miles	2.59	square kilometers	km^2
		VOLUME		
fl oz	fluid ounces	29.57	milliliters	mL
gal	gallons	3.785	liters	L
ft^3	cubic feet	0.028	cubic meters	m^3
yd^3	cubic yards	0.765	cubic meters	m^3
	NOTE: volumes greater than 1000 L shall be shown in m^3			
		MASS		
oz	ounces	28.35	grams	g
lb	pounds	0.454	kilograms	kg
T	short tons (2000 lb)	0.907	megagrams (or "metric ton")	Mg (or "t")
		TEMPERATURE (exact degrees)		
°F	Fahrenheit	5 (F-32)/9 or (F-32)/1.8	Celsius	°C
		ILLUMINATION		
fc	foot-candles	10.76	lux	lx
fl	foot-Lamberts	3.426	$candela/m^2$	cd/m^2
		FORCE and PRESSURE or STRESS		
lbf	poundforce	4.45	newtons	N
lbf/in^2	poundforce per square inch	6.89	kilopascals	kPa

APPROXIMATE CONVERSIONS FROM SI UNITS

Symbol	When You Know	Multiply By	To Find	Symbol
		LENGTH		
mm	millimeters	0.039	inches	in
m	meters	3.28	feet	ft
m	meters	1.09	yards	yd
km	kilometers	0.621	miles	mi
		AREA		
mm^2	square millimeters	0.0016	square inches	in^2
m^2	square meters	10.764	square feet	ft^2
m^2	square meters	1.195	square yards	yd^2
ha	hectares	2.47	acres	ac
km^2	square kilometers	0.386	square miles	mi^2
		VOLUME		
mL	milliliters	0.034	fluid ounces	fl oz
L	liters	0.264	gallons	gal
m^3	cubic meters	35.314	cubic feet	ft^3
m^3	cubic meters	1.307	cubic yards	yd^3
		MASS		
g	grams	0.035	ounces	oz
kg	kilograms	2.202	pounds	lb
Mg (or "t")	megagrams (or "metric ton")	1.103	short tons (2000 lb)	T
		TEMPERATURE (exact degrees)		
°C	Celsius	1.8C+32	Fahrenheit	°F
		ILLUMINATION		
lx	lux	0.0929	foot-candles	fc
cd/m^2	$candela/m^2$	0.2919	foot-Lamberts	fl
		FORCE and PRESSURE or STRESS		
N	newtons	0.225	poundforce	lbf
kPa	kilopascals	0.145	poundforce per square inch	lbf/in^2

TABLE OF CONTENTS

LIST OF FIGURES

LIST OF TABLES

LIST OF ABBREVIATIONS AND SYMBOLS

Abbreviations

AASHTO	American Association of State Highway and Transportation Officials
ADT	Average Daily Traffic
BAM	Bridge Asset Management
CB	Condition-based
BCR	Benefit-Cost Ratio
CR	Condition Rating
DDPG	Deep Deterministic Policy Gradient
DOT	Department of Transportation
DQN	Deep Q Network
DRL	Deep Reinforcement Learning
DS	Damage State
FHWA	Federal Highway Administration
IM	Intensity Measure
LHS	Latin hypercube sampling
med	Median
NBI	National Bridge Inventory
NCHRP	National Cooperative Highway Research Program
P-DRL	Parameterized Deep Reinforcement Learning
PGA	Peak Ground Acceleration
P-PERDQN	Parameterized Prioritized Experience Replay Deep Q Network
RL	Reinforcement Learning
SNBI	Specifications for the National Bridge Inventory
TAMP	Transportation Asset Management Plan
TD	Temporal Difference

Symbols

A	Action space
a	Specific action
β_s	Safety cost multiplier
C_O	Operation cost

C_T	Time loss cost
C_{TC}	Time-cumulative cost
C_W	Hourly wage
D	Replay buffer
L	Detour length
O_{car}	Average occupancy per car
$Q(.)$	Action-value function
r_{truck}	Ratio of truck traffic
R	Long term cumulative reward
r	Instant annual reward
S	State space
s	Specific state
T	Planning time horizon
t	Time step
V	Average detour speed
P	Probability
$\boldsymbol{P}$	Transition Probability Matrix
$\boldsymbol{x}$	Bridge parameters
α	Residual traffic carrying capacity ratio
γ	Discount factor
λ	Annual rate of exceedance
ξ	Dispersion
$\pi(.)$	Maintenance policy
Φ	Standard normal cumulative distribution function
ϕ	Traffic carrying capacity ratio

Executive Summary

This project develops a methodology for risk-based multi-threat decision-support to inform long-term bridge asset management of a portfolio of bridges, with a particular focus on chronic aging-induced condition deterioration in conjunction with more abrupt and extreme natural hazard (e.g., earthquakes) impacts. Particularly, in Phase 1 of this project, a decision-support tool for maintenance planning at the individual bridge level is developed, including three modules: (1) a stochastic simulation module to model the bridge condition transitions; (2) a life-cycle cost estimation module translating the bridge conditions and intervention actions to monetary costs; and (3) an AI-informed decision-support module for optimal bridge maintenance and retrofit planning. The resulting decision-support tool can offer adaptive and proactive sequential maintenance decisions given a bridge's current conditions and key attributes (e.g., deck area, average daily traffic volume), with the goal to minimize the cumulative costs over a prolonged planning horizon. It is anticipated that the proposed research will facilitate more cost-effective bridge asset management.

The bridge condition deterioration is first modeled to holistically capture the bridge degradation due to multiple external stressors (e.g., aging deterioration, seismic hazard, and extreme weather events). Each individual bridge structure is abstracted into a structural system comprised of three general bridge components, namely deck, superstructure, and substructure. To separate the influences from aging-induced chronical degradation and seismic hazard, and to also consider the interactions between the two sources of threats, the bridge states are divided into two categories, namely condition ratings of bridge components according to the National Bridge Inventory (NBI) definitions, and system-level seismic damage states (i.e., none, slight, moderate, extensive, and complete). Annual probabilistic condition transitions are modeled via Markov chains, where different Markov state transition probability matrices are considered to model the state transitions for the three bridge components under aging deterioration and under different types of component-level maintenance actions (i.e., minor maintenance, major maintenance, and replacement). Besides, bridge system-level seismic fragility and risk modeling is introduced to capture the effect of seismic hazard and seismic retrofit actions. Annual seismic damage occurrence probabilities are derived by convolving seismic hazard curves with the fragility models, followed by damage state random sampling to obtain the bridge system-level damage states during any annual transition. The impact of seismic damage on the bridge component condition ratings is captured by employing a decision-tree based approach to update the condition ratings of the three generic bridge components based on the system-level seismic damage states.

Based on the above integrated and probabilistic bridge condition and seismic damage simulation environment, monetary costs (direct and indirect cost) are estimated by considering the costs incurred due to multiple factors, including condition deterioration and intervention actions in a life-cycle context. Specifically, maintenance cost and seismic retrofit cost are considered as the direct costs. Indirect costs that reflect the socioeconomic consequences due to the interruption to the bridges' traffic carrying capabilities are considered, including: (1) vehicle operation cost; (2) time costs to passengers and trucks; and (3) safety cost. The direct and indirect costs are combined into the total annual costs, which are then aggregated to obtain the life-cycle cumulative costs by

considering a discount factor to capture the compound effect of depreciation and inflation throughout the planning horizon. In addition, a preliminary benefit-cost analysis is conducted to evaluate the effectiveness of various seismic retrofit strategies for two geographical locations (Memphis and San Francisco) with different levels of seismic hazard.

Leveraging the previously developed modules for the bridge condition deterioration, seismic risk, and life-cycle cost estimations, Deep Reinforcement Learning (DRL), an artificial intelligence (AI) technique, is introduced to identify proactive and risk-aware policies for sequential maintenance decision making for a portfolio of highway bridges. The proposed DRL-based policy is parameterized by taking bridge-specific attributes, such as total deck area, average daily traffic volume, truck traffic ratio, and detour length, as inputs and can flexibly accommodate the decision needs for various individual bridges within a bridge portfolio. To ensure that the policies developed for bridge management comply with real-world practices, a set of practical action constraints are introduced. The portfolio-level DRL policies are found to exhibit satisfactory performance when applied to different individual bridges. At the bridge portfolio-level, the portfolio-level DRL policies significantly outperform other conventional condition-based policies. To further improve the trustworthiness of the AI policies, decision visualization and reasoning tools are also developed so that human decision makers can be more aware of the long-term benefits among different candidate intervention actions. In addition, the effect of human overriding the decisions suggested by the AI agent is also investigated, by mixing the DRL-based policy with a condition-based policy with different mixture probabilities. The results reveal that the AI-based policy is highly robust to potential human override. In addition, random episode realizations are presented to demonstrate the random life-cycle condition rating and maintenance action trajectories of select case study bridges. These realizations serve to demonstrate how the DRL-based policies can be practically applied, showcasing their dynamic and adaptable nature. Finally, the efficacy of seismic retrofitting when coupled with the AI-based maintenance decision policy is investigated. Findings indicate that both seismic damage and retrofitting interventions impact the life cycle cost of bridges, particularly in regions susceptible to frequent seismic events, and more realistic benefit-cost analysis can be achieved to evaluate the efficacy of seismic retrofit.

In summary, the developed tool is highly modular that it can utilize existing data (e.g., the NBI data) and models (e.g., Markovian state transition matrices for bridge conditions, fragility models, life-cycle cost estimation), and can be seamlessly integrated into the state-of-practice for bridge asset management with great potential for user customization. The developed AI-informed sequential decision-making tool holistically incorporates domain knowledge regarding probabilistic bridge deterioration, risk quantification, and life-cycle cost estimation, offering proactive, adaptive, and long-term focused maintenance planning for various individual bridges within a bridge portfolio. This decision-support tool can provide more informed decision suggestions, greatly alleviate the decision burden for practitioners, and facilitate more effective bridge asset management to better preserve the nation's highway bridge asset.

CHAPTER 1. INTRODUCTION

Though vital to America's economy, the U.S. bridge infrastructure only received a rating of C according to the 2021 ASCE Infrastructure Report Card [1]. Currently 42% of the nation's bridges are 50 years (the design service life of most bridges) or older; nearly 231,000 bridges need repair and preservation work; and 7.5% of all the bridges are structurally deficient. The bridge infrastructure systems have been underfunded with a staggering $125 billion bridge repair backlog, and the rate of repair, rehabilitation, and replacement is surpassed by the rate of deterioration. In addition, there has been an accelerating trend of bridges transitioning from the "Good" to "Fair" condition in recent years [1]. Moreover, bridge assets are also facing ever-increasing traffic demand due to urbanization and are exposed to multiple extreme natural hazards occurring with different frequencies and intensities that degrade their structural performance and functionality.

Most of the existing bridge asset management (BAM) plans are still heuristic and need to be enhanced with more comprehensive, systematic, and adaptive decision policies. To tackle these research gaps, this project aims to propose an integrated risk-based decision-support tool, by leveraging probabilistic multi-threat life-cycle analysis and advanced AI-informed decision-support tools. The proposed methodology is highly modular and can fully exploit commonly available input data, thereby flexibly adapting to the needs of local transportation agencies (e.g., state DOTs) to facilitate more informed and cost-effective BAM.

The goal of this project is to develop a risk-based multi-threat decision-support methodology for BAM, through holistic incorporation of uncertainties and impacts from environmental and natural hazard threats and intervention actions, while minimizing the long-term monetary costs. Phase 1 of this project consists of three closely integrated research tasks, respectively addressing (1) multi-threat bridge performance modeling; (2) risk-based life-cycle cost analysis; and (3) artificial intelligence (AI) informed sequential decision-support for bridge portfolios as shown in **Figure 1-1**. The proposed methodology will lead to a paradigm shift in BAM from the heuristic, qualitative, and subjective legacy management practice to a more systematic, quantitative, and risk-based fashion.

Following the introductory chapter, in Chapter 2, the bridge condition deterioration is modeled to holistically capture the bridge degradation due to multiple external stressors (e.g., aging deterioration and seismic hazard). In Chapter 3, based on the above integrated and probabilistic bridge condition modeling approach, monetary costs (direct and indirect cost) are estimated by considering the costs incurred due to multiple factors, including condition deterioration and intervention actions in a life-cycle context. In Chapter 4, based on the previously developed modules for the bridge condition deterioration, and life-cycle cost estimations, Deep Reinforcement Learning (DRL), an artificial intelligence (AI) technique, is introduced and evaluated to provide adaptive and risk-aware decision-support for sequential maintenance planning for a portfolio of highway bridges. Chapter 5 summarizes the work and the key findings of this research. Appendix A provides detailed elaboration of the DRL algorithms, and Appendix B lists the key assumptions of the proposed decision-support tool, along with inputs that can be customized based on the users' need. Appendix C provides instructions on how to use the open-source computer codes to train and test the AI decision agents.

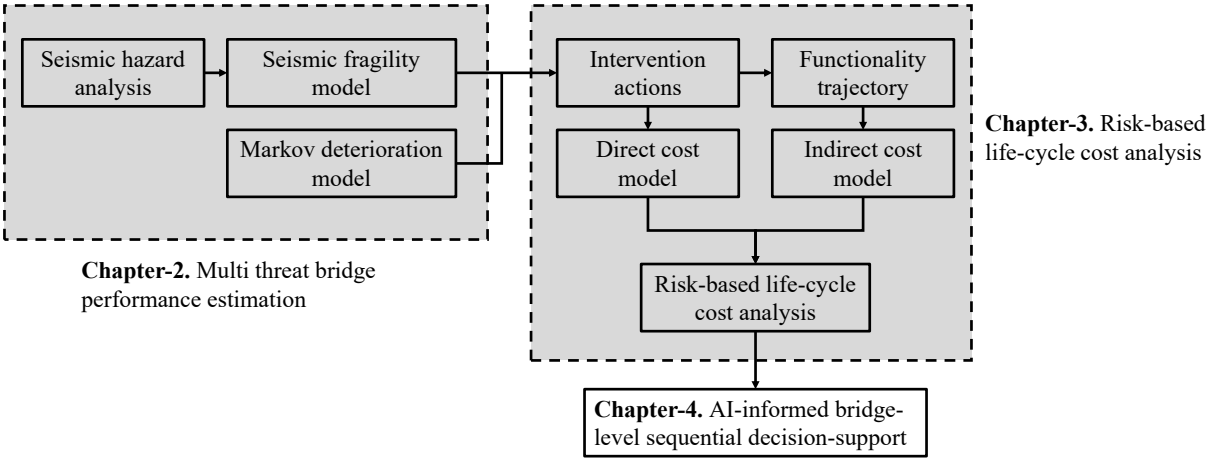

Figure 1-1. Overview of research tasks of the integrated risk-based multi-threat long-term bridge asset management framework

CHAPTER 2. MULTI-THREAT BRIDGE PERFORMANCE ESTIMATION

2.1. Introduction

Stochastic bridge condition evolution will be modeled in this chapter to holistically capture the bridge condition variation due to multiple external stressors (i.e., aging deterioration and seismic hazard) and intervention actions. Deterioration models aiming at capturing the degradation of bridge component conditions can be generally classified into regression-based and Markov-based models. Regression-based models are typically developed by conducting regression analysis using statistical regression or machine learning techniques on recorded bridge condition data (e.g., the NBI condition ratings) [2,3]. Regression-based models can incorporate multiple predictor variables and offer powerful predictive performance. However, these models are typically deterministic and not robust enough to flexibly accommodate effect of intervention actions on the bridges. Markov based models are probabilistic and state-based models, where the states are typically discrete conditions of the bridge components [4–6]. With the commonly adopted homogeneous Markov chain assumption, the next state only depends only on the current state, and the probability of transitioning to the next state is specified by Markov state transition matrices. Owing to the abundance of the NBI condition data, Markov based models have received prevalent research attention and have been adopted in many existing bridge asset management software (e.g., Pontis [7] and AASHTOWare [8]). Moreover, the state-based and probabilistic nature of Markov-based models also naturally fit into the Markov decision process later to be introduced in Chapter 4. For this reason, Markov based models will be employed for the bridge condition modeling in this research. However, it should be noted that these Markov models may not be able to accurately characterize the deterioration of bridge conditions under non-stationary conditions.

Natural hazard (e.g., earthquakes, floods) fragility and risks of highway bridges are also of critical concerns. Although earthquake hazard is considered in this research, the proposed methodology can also be extended to accommodate other types of natural hazard provided the related hazard curves and fragility models are available. In the context of earthquake impact on highway bridges, there exists a large body of research in seismic fragility modeling of pristine highway bridges [9–13], as well as in the seismic fragility modeling of aging bridges [14–16].

Nevertheless, there is a lack of research effort in integrating both bridge condition deterioration and seismic risks in life-cycle analysis, with the capability to flexibility accommodate the effect of maintenance actions and seismic retrofit and repairs. To address the above-mentioned research gaps, in the following sections, a multi-threat bridge performance modeling module will be developed.

2.2. Overview of the Multi-Threat Bridge Performance Modeling

Within this module, each individual bridge structure is abstracted into a structural system comprised of multiple bridge components. To separate the influences from aging-induced chronical degradation and seismic hazard, and to also consider the interactions between the two sources of threats, the bridge states are divided into two categories, namely condition ratings of generic bridge components (i.e., deck, superstructure, and substructure) according to the NBI, and system-level seismic damage states determined according to HAZUS [17].

The overview flowchart of the proposed multi-threat bridge performance modeling module is shown in **Figure 2-1**. Particularly, this module will provide a probabilistic means to characterize the bridge condition and seismic damage transitions from the previous year to the next year. Bridge condition deterioration, seismic fragility and damage, as well as any bridge intervention actions related to maintenance and seismic retrofit that occurred during each annual decision interval will be synergistically captured. This annual bridge condition and damage state modeling module will then serve as the building block in the AI-based life-cycle decision making tool to be introduced in Chapter 4. The major components and their connection within this module are introduced as follows.

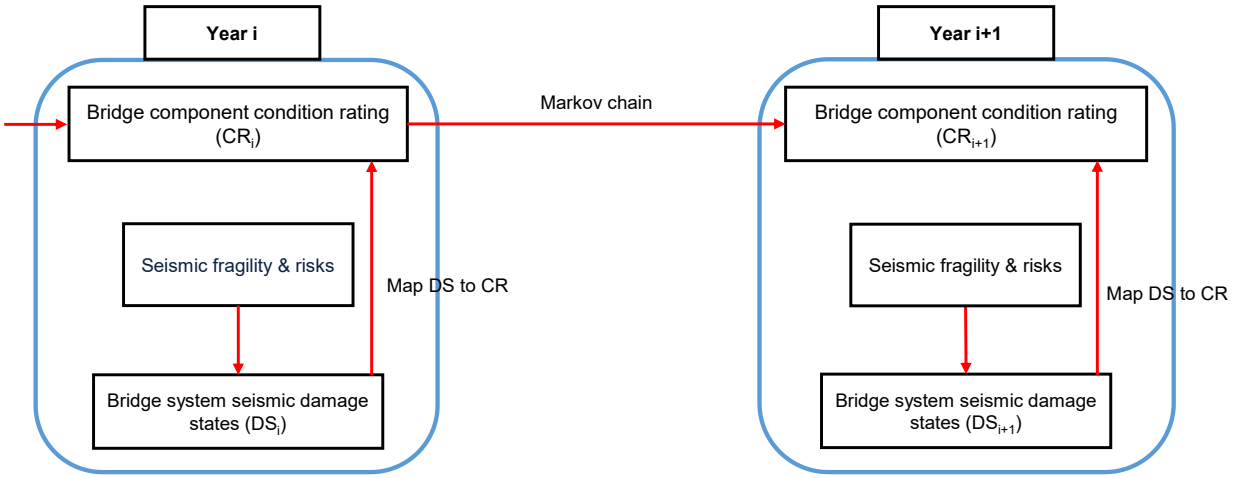

Figure 2-1. Overview flowchart of Chapter 2

2.3. Bridge Condition Deterioration Modeling

2.3.1. Bridge Component Condition Ratings

The NBI [18] bridge condition ratings are considered to reflect the degradation of bridge component conditions due chronical aging deterioration. Although the NBI condition ratings are global condition metrics of generic bridge components such as decks, superstructures, and substructures, they are selected mainly because of their prevalent application in state DOT practice and data availability nationwide. The NBI database has the most comprehensive records of bridge conditions in the U.S., fostering the development of many bridge condition deterioration models [19–22], which are essential parts to enable the decision-support models later introduced in Chapter 4. It should be noted that the proposed modeling module can also be adapted to accommodate other more sophisticated bridge condition evaluation metrics such as the element-level condition data, which provides more refined information related to both the quantities and conditions of the bridge components. Three types of bridge components, including deck, superstructure, and substructure are considered. The NBI condition rating definitions along with the correspondence to the FHWA general condition categories (i.e., Good/Fair/Poor) are shown in **Table 2-1**.

Table 2-1. NBI condition ratings for bridge components [23]

Code	Description	FHWA Good/Fair/Poor
N	N/A	N/A
9	Excellent condition	Good
8	Very good condition—no problems noted	
7	Good condition—some minor problems	
6	Satisfactory condition—structural elements show some minor deterioration	Fair
5	Fair condition—all primary structural elements are sound but may have minor section loss, cracking, spalling or scour	
4	Poor condition—advanced section loss, deterioration, spalling or scour	Poor
3	Serious condition—loss of section, deterioration of primary structural elements. Fatigue cracks in steel or shear cracks in concrete may be present	
2	Critical condition—advanced deterioration of primary structural elements. Fatigue cracks in steel or shear cracks in concrete may be present or scour may have removed substructure support. Unless closely monitored it may be necessary to close the bridge until corrective action is taken	
1	Imminent failure condition—major deterioration or section loss present in critical structural components or obvious vertical or horizontal movement affecting structure stability. Bridge is closed to traffic but corrective action may put it back in light service	
0	Failed condition—out of service; beyond corrective action	

2.3.2. Development of Component-Level Markovian Transition Matrices Under Do-Nothing Scenarios

For demonstration purposes, Markov state transition probability matrices for the three bridge components (deck, superstructure, and substructure) under chronic aging deterioration (i.e., do-nothing) based on the Tennessee NBI data. These matrices are derived using NBI condition rating (CR) data collected from 1992 to 2021. Since the focus here is on developing Markov matrices for the "do-nothing" scenarios, data entries with CR improvement are neglected. Note that CR = 0 is

merged into CR = 1 as the associated data samples are very limited. The transition matrices for each component are calculated using the following equation:

$$P_{ij} = \frac{n_{ij}}{\sum_{k=1}^{9} n_{ik}} \tag{2-1}$$

where: P_{ij} (i.e., the entry on the i^{th} row and the j^{th} column) denotes the transition probability from CR i to j, and n_{ij} is the number of transition occurrence from CR i to j. The derived Markov transition matrices for the three bridges components under "do-nothing" are given as follows:

$$\begin{array}{c} (i) \\ \boldsymbol{P}_{DECK} = \end{array} \begin{array}{c} \begin{array}{ccccccccc} 1 & 2 & 3 & 4 & 5 & 6 & 7 & 8 & 9 \end{array} \quad (j) \\ \begin{bmatrix} 1.00 & 0.00 & 0.00 & 0.00 & 0.00 & 0.00 & 0.00 & 0.00 & 0.00 \\ 0.00 & 1.00 & 0.00 & 0.00 & 0.00 & 0.00 & 0.00 & 0.00 & 0.00 \\ 0.00 & 0.00 & 1.00 & 0.00 & 0.00 & 0.00 & 0.00 & 0.00 & 0.00 \\ 0.00 & 0.00 & 0.0114 & 0.9886 & 0.00 & 0.00 & 0.00 & 0.00 & 0.00 \\ 0.00 & 0.00 & 0.00 & 0.0174 & 0.9826 & 0.00 & 0.00 & 0.00 & 0.00 \\ 0.00 & 0.00 & 0.00 & 0.00 & 0.0227 & 0.9773 & 0.00 & 0.00 & 0.00 \\ 0.00 & 0.00 & 0.00 & 0.00 & 0.00 & 0.0268 & 0.9732 & 0.00 & 0.00 \\ 0.00 & 0.00 & 0.00 & 0.00 & 0.00 & 0.00 & 0.0714 & 0.9286 & 0.00 \\ 0.00 & 0.00 & 0.00 & 0.00 & 0.00 & 0.00 & 0.0452 & 0.1011 & 0.8537 \end{bmatrix} \begin{array}{c} 1 \\ 2 \\ 3 \\ 4 \\ 5 \\ 6 \\ 7 \\ 8 \\ 9 \end{array} \end{array} \tag{2-2}$$

$$\boldsymbol{P}_{Super} = \begin{bmatrix} 1.00 & 0.00 & 0.00 & 0.00 & 0.00 & 0.00 & 0.00 & 0.00 & 0.00 \\ 0.0282 & 0.9718 & 0.00 & 0.00 & 0.00 & 0.00 & 0.00 & 0.00 & 0.00 \\ 0.00 & 0.0107 & 0.9893 & 0.00 & 0.00 & 0.00 & 0.00 & 0.00 & 0.00 \\ 0.00 & 0.00 & 0.0147 & 0.9853 & 0.00 & 0.00 & 0.00 & 0.00 & 0.00 \\ 0.00 & 0.00 & 0.00 & 0.0194 & 0.9806 & 0.00 & 0.00 & 0.00 & 0.00 \\ 0.00 & 0.00 & 0.00 & 0.00 & 0.0246 & 0.9754 & 0.00 & 0.00 & 0.00 \\ 0.00 & 0.00 & 0.00 & 0.00 & 0.00 & 0.0276 & 0.9724 & 0.00 & 0.00 \\ 0.00 & 0.00 & 0.00 & 0.00 & 0.00 & 0.00 & 0.0532 & 0.9468 & 0.00 \\ 0.00 & 0.00 & 0.00 & 0.00 & 0.00 & 0.00 & 0.0282 & 0.0995 & 0.8723 \end{bmatrix} \tag{2-3}$$

$$\boldsymbol{P}_{Sub} = \begin{bmatrix} 1.00 & 0.00 & 0.00 & 0.00 & 0.00 & 0.00 & 0.00 & 0.00 & 0.00 \\ 0.00 & 1.00 & 0.00 & 0.00 & 0.00 & 0.00 & 0.00 & 0.00 & 0.00 \\ 0.00 & 0.0142 & 0.9858 & 0.00 & 0.00 & 0.00 & 0.00 & 0.00 & 0.00 \\ 0.00 & 0.00 & 0.0208 & 0.9792 & 0.00 & 0.00 & 0.00 & 0.00 & 0.00 \\ 0.00 & 0.00 & 0.00 & 0.0302 & 0.9698 & 0.00 & 0.00 & 0.00 & 0.00 \\ 0.00 & 0.00 & 0.00 & 0.00 & 0.0282 & 0.9718 & 0.00 & 0.00 & 0.00 \\ 0.00 & 0.00 & 0.00 & 0.00 & 0.00 & 0.0207 & 0.9793 & 0.00 & 0.00 \\ 0.00 & 0.00 & 0.00 & 0.00 & 0.00 & 0.00 & 0.0654 & 0.9346 & 0.00 \\ 0.00 & 0.00 & 0.00 & 0.00 & 0.00 & 0.00 & 0.0349 & 0.0925 & 0.8726 \end{bmatrix} \tag{2-4}$$

2.3.3. Development of Component-level Markovian Transition Matrices for Different Maintenance Actions

The effect of maintenance actions should also be incorporated, as these intervention actions may preserve or improve the bridge component conditions. **Table 2-2** lists the maintenance action

definitions based on the FHWA Bridge Preservation Guide [23], where four major categories of maintenance actions are outlined including cyclic maintenance, condition-based maintenance, rehabilitation, and total bridge replacement. Since this research adopts a component-based approach where the conditions and maintenance actions will be specifically considered for each of the three bridge components, three high-level component-level maintenance actions are considered including: minor maintenance (or condition-based maintenance), major maintenance (or rehabilitation), and replacement (or rebuild).

Table 2-2. Maintenance actions based on Bridge Preservation Guide [23]

Category		Treatments
Preventive Maintenance	**Cyclical**	Wash/clean bridge decks or entire bridge Install deck overlay on concrete decks Seal concrete decks with waterproofing penetrating sealant Zone coat steel beam/girder ends Lubricate bearing devices
	Condition-based	Drains, Repair/Replace Joint Seal Replacement Joint Repair/Replace/Elimination Electrochemical Extraction (ECE)/Cathodic Protection (CP) Concrete Deck Repair (see halo effect below) in Conjunction with Overlays, CP Systems or ECE Treatment Drains, Repair/Replace Deck Overlays (thin polymer epoxy, asphalt with waterproof membrane, rigid overlays) Repair/Replace Approach Slabs Seal/Patch/Repair Superstructure Concrete Protective Coat Concrete/Steel Elements Spot/Zone/Full Painting Steel Elements Steel Member Repair Fatigue Crack Mitigation (pin-and-hanger replacement, retrofit fracture critical members) Bearing Restoration (cleaning, lubrication, resetting, replacement) Movable Bridge Machinery Cleaning/Lubrication/Repair Patch/Repair Substructure Concrete Protective Coat/Concrete/Steel Substructure ECE/CP Spot/Zone/Full Painting Steel Substructure Pile Preservation (jackets/wraps/CP) Channel Cleaning / Debris Removal Scour Countermeasure (installation/repair)
Rehabilitation		Partial or complete deck replacement Superstructure replacement strengthening
Replacement		Total replacement of an existing bridge

Due to the lack of well-organized and publicly-available bridge maintenance record data (compared with the wide availability of the NBI condition data), only limited research efforts [24] have been committed to developing Markov matrices to characterize the effect of maintenance actions. In the absence of quality data, component-level Markovian transition matrices under different maintenance actions are usually obtained via expert judgment [25,26]. Aiming at obtaining reasonable estimates of Markov matrices for maintenance actions, the research team

consulted multiple information sources, including the FHWA bridge preservation guide [23], state Transportation Asset Management Plans (TAMPs) [27–29], technical reports (e.g., [30]), and bridge maintenance record [24], and the resulting Markov transition matrices are synthesized as shown in Eqs. (2-5) to (2-7). It should be noted that users can reassign the Markov transition matrices based on their own experience or in-house data. It is assumed that the three generic bridge components share the same transition probability matrices under maintenance actions other than "Do nothing". Since the condition-based maintenance actions are typically applied to components in a "Good" or "Fair" condition with limited effect in improving the condition ratings, it is assumed that the minor maintenance actions are only effective for CR > 4 (i.e., above the "Poor" condition). Since rehabilitation actions are mostly enforced on components in a "Poor" condition (i.e., CR ≤ 4), it is assumed that the major maintenance actions are effective for CR > 2, with better effects of condition improvement of up to two ratings. It should be noted that these Markov matrices can be further modified or refined by exploiting the maintenance record data collected by state DOTs. Moreover, additional bridge maintenance record data will soon be included into the NBI database according to the Specifications for the National Bridge Inventory (SNBI) [31] and improved estimates of Markov transition matrices under different maintenance actions can be expected.

$$\boldsymbol{P}_{Minor} = \begin{bmatrix} 1 & 0 & 0 & 0 & 0 & 0 & 0 & 0 & 0 \\ 0 & 1 & 0 & 0 & 0 & 0 & 0 & 0 & 0 \\ 0 & 0 & 1 & 0 & 0 & 0 & 0 & 0 & 0 \\ 0 & 0 & 0 & 1 & 0 & 0 & 0 & 0 & 0 \\ 0 & 0 & 0 & 0 & 0.9 & 0.1 & 0 & 0 & 0 \\ 0 & 0 & 0 & 0 & 0 & 0.8 & 0.2 & 0 & 0 \\ 0 & 0 & 0 & 0 & 0 & 0 & 0.7 & 0.3 & 0 \\ 0 & 0 & 0 & 0 & 0 & 0 & 0 & 0.6 & 0.4 \\ 0 & 0 & 0 & 0 & 0 & 0 & 0 & 0 & 1 \end{bmatrix} \tag{2-5}$$

$$\boldsymbol{P}_{Major} = \begin{bmatrix} 1 & 0 & 0 & 0 & 0 & 0 & 0 & 0 & 0 \\ 0 & 1 & 0 & 0 & 0 & 0 & 0 & 0 & 0 \\ 0 & 0 & 0.3 & 0.4 & 0.3 & 0 & 0 & 0 & 0 \\ 0 & 0 & 0 & 0.1 & 0.3 & 0.6 & 0 & 0 & 0 \\ 0 & 0 & 0 & 0 & 0.1 & 0.2 & 0.7 & 0 & 0 \\ 0 & 0 & 0 & 0 & 0 & 0.05 & 0.1 & 0.85 & 0 \\ 0 & 0 & 0 & 0 & 0 & 0 & 0.05 & 0.05 & 0.9 \\ 0 & 0 & 0 & 0 & 0 & 0 & 0 & 0.02 & 0.98 \\ 0 & 0 & 0 & 0 & 0 & 0 & 0 & 0 & 1 \end{bmatrix} \tag{2-6}$$

$$P_{Replacement} = \begin{bmatrix} 0 & 0 & 0 & 0 & 0 & 0 & 0 & 0 & 1 \\ 0 & 0 & 0 & 0 & 0 & 0 & 0 & 0 & 1 \\ 0 & 0 & 0 & 0 & 0 & 0 & 0 & 0 & 1 \\ 0 & 0 & 0 & 0 & 0 & 0 & 0 & 0 & 1 \\ 0 & 0 & 0 & 0 & 0 & 0 & 0 & 0 & 1 \\ 0 & 0 & 0 & 0 & 0 & 0 & 0 & 0 & 1 \\ 0 & 0 & 0 & 0 & 0 & 0 & 0 & 0 & 1 \\ 0 & 0 & 0 & 0 & 0 & 0 & 0 & 0 & 1 \\ 0 & 0 & 0 & 0 & 0 & 0 & 0 & 0 & 1 \end{bmatrix} \tag{2-7}$$

2.4. Seismic Fragility Modeling and Risk Assessment

Bridge seismic fragility modeling and risk assessment is a vital part to evaluate bridge seismic vulnerability. In this section, system-level bridge seismic fragility models will be leveraged and will be convolved with seismic hazard curves to obtain the unconditional seismic risk and damage estimates.

2.4.1. Seismic Fragility Modeling

The general functional form of the system-level seismic fragility model is shown in Eq. (2-8), which gives the probability of exceeding a certain seismic damage state (DS) conditioned on a ground motion intensity measure (IM).

$$P(DS|IM) = \Phi\left(\frac{ln\,(IM) - ln(med_{sys})}{\xi_{sys}}\right) \tag{2-8}$$

where med_{sys} is the median value (in unit of g) of system capacity for each DS, and ξ_{sys} is the dispersion, or logarithmic standard deviation of the fragility model. The commonly adopted Peak Ground Acceleration (PGA) is considered herein as the IM. $\Phi(.)$ is the standard normal cumulative distribution function. **Table 2-3** presents the fragility models adopted from Padgett et al. (2010) [32] for the four damage states for as-built Multi-Span Simply Supported (MSSS) concrete bridge as case study for demonstration purpose. It is noted that system fragility parameter for other bridge types can be found in Padgett et al. (2010) [32].

Table 2-3. System fragility parameters (in units of g) for each damage state [32]

Damage state	**Slight**		**Moderate**		**Extensive**		**Complete**	
	med_{sys}	ξ_{sys}	med_{sys}	ξ_{sys}	med_{sys}	ξ_{sys}	med_{sys}	ξ_{sys}
Fragility parameters	0.21	0.69	0.61	0.60	0.86	0.60	1.20	0.61

Besides the maintenance actions for the three generic bridge components (i.e., deck, superstructure, and substructure), several seismic retrofit actions, including: (1) steel column jackets; and (2) seat extenders for girder and bent beams; (3) shear key for bent beams and abutment, and a set of retrofit combinations are also considered in this study. As presented in **Table 2-4**, the effects of these retrofit actions are considered via modification factors to the as-built seismic fragility model parameters. These modification factors are used to scale the median values of the as-built fragility model to reflect the reduced seismic damage probability after implementing these retrofits, and it is assumed that the retrofit actions will not affect the fragility model dispersions. It is noteworthy that some retrofit actions may slightly increase the seismic vulnerability (e.g., shear key for the moderate damage state). This is because the median value modification factors, as outlined in **Table 2-4**, are based on system-level considerations, where enhancing one component might affect the seismic fragility of other related bridge components. The fragility modification factors for other bridge classes can be found in [32]**.**

Table 2-4. Median value modification factors for MSSS concrete bridge adapted from [32]

Retrofit measure	Slight	Moderate	Extensive	Complete
Steel Jacketing (SJ)	1.03	1.16	1.17	1.20
Seat Extender (SE)	1.01	1.00	1.00	1.31
Shear Key (SK)	1.01	0.98	0.99	1.01
SE + SK	1.01	0.97	0.99	1.37
SJ + SE + SK	1.03	1.16	1.17	1.37

Figure 2-2 shows the fragility curves for exceeding different system-level seismic damage states before and after multi-retrofitting (i.e., SJ+SE+SK). It is obvious that the probability of exceedance decreases especially for the moderate to complete damage states.

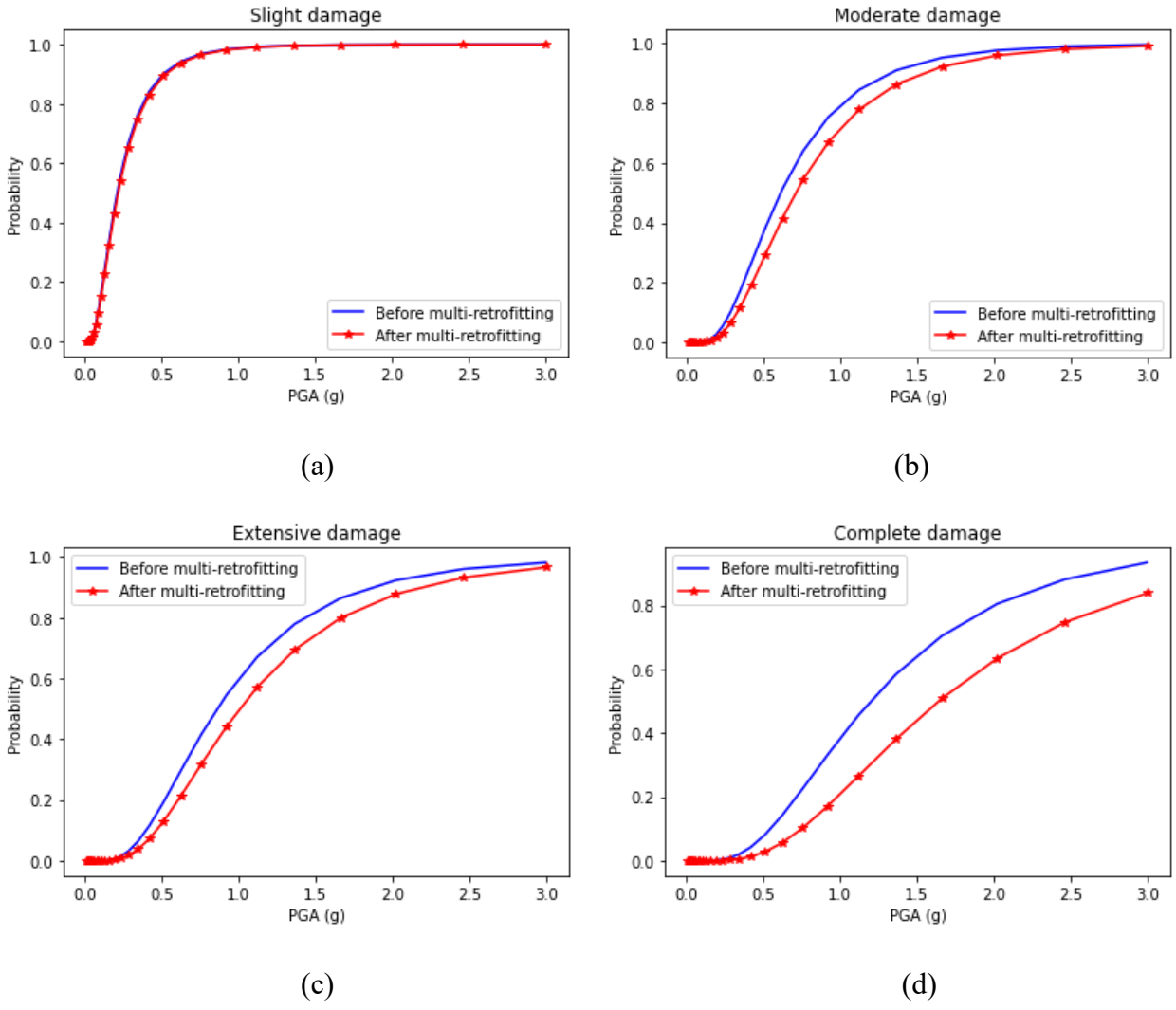

Figure 2-2. Change in system fragility due to multi-retrofitting for different damage states: (a) Slight, (b) Moderate, (c) Extensive, (d) Complete

2.4.2. Annual Seismic Damage Risk Derivation and Damage State Sampling

After obtaining the seismic fragility functions, the annual seismic risk of the bridge system can be estimated according to Eq. (2-9). The users provide site-specific seismic hazard information in the form of a seismic hazard curve conditioned on a specific IM. The annual rate of exceeding a certain damage state (DS) can be calculated as follows:

$$\lambda_{annual}(DS) = \int_{IM} P(DS|IM) \left|\frac{d\lambda(IM)}{dIM}\right| dIM \quad (2\text{-}9)$$

where $\lambda(IM)$ denotes the annual rate of exceeding a certain IM, which is available from site-specific seismic hazard curves. Seismic hazard curves are publicly available through the United States Geological Survey (USGS) Unified Hazard Tool (https://earthquake.usgs.gov/hazards/interactive/), or can be derived from site-specific probabilistic seismic hazard analysis via OpenSHA [33] or OpenQuake [34]. For demonstration purposes, the seismic hazard curve for PGA for a site in Memphis is extracted from the USGS Unified Hazard Tool as shown in Figure 2-3.

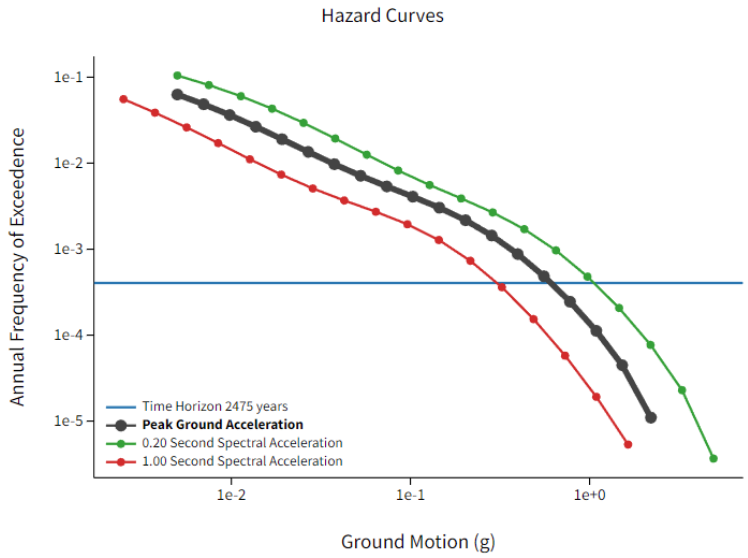

Figure 2-3. Hazard curve for a site in Memphis from the USGS Unified Hazard Tool (https://earthquake.usgs.gov/hazards/interactive/)

The risk integral in Eq. (2-9) is evaluated numerically, by discretizing it into the summation of risk contributions from multiple IM levels as follows:

$$\lambda_{annual}(DS) = \sum_i P(DS|IM_i) \left|\frac{d\lambda(IM_i)}{dIM_i}\right| \Delta IM_i \quad (2\text{-}10)$$

where within each IM level, the fragility estimates $P(DS|IM_i)$ corresponding to this IM level will be evaluated, $\left|\frac{d\lambda(IM_i)}{dIM_i}\right|$ is the absolute value of the hazard curve slope at IM_i, and ΔIM_i is the IM interval. To facilitate more efficient and accurate calculation of the hazard curve slope, a hyperbolic function is fitted to the hazard curve data according to [35], as follows:

$$\hat{v} = a \cdot exp\left[b\left(Ln\left(\frac{PGA}{\gamma}\right)\right)^{-1}\right] \tag{2-11}$$

In this case, Eq. (2-11) optimized using the Memphis data in which the coefficients derived as follows: $a = 11.82, b = 56.16, \gamma = 134.72$, and the comparison of the original USGS hazard curve and the fitted hazard curve is shown in Figure 2-4.

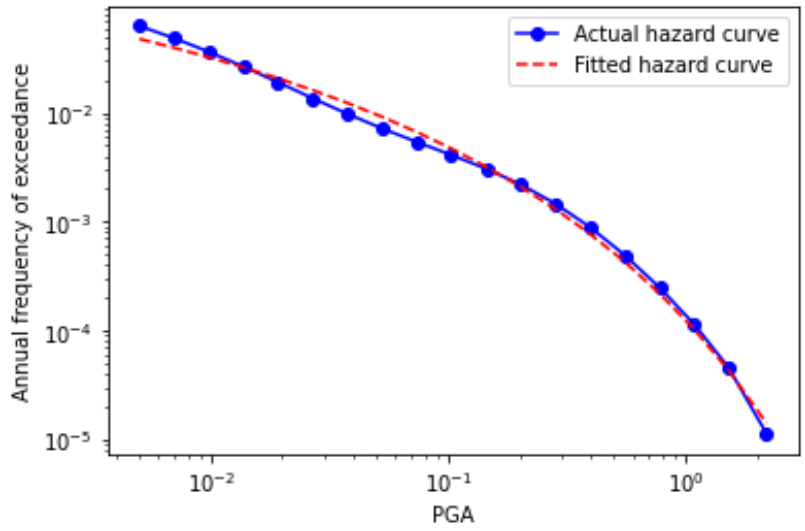

Figure 2-4. Comparison of the USGS hazard curve and the fitted hazard curve for PGA

Under the homogenous Poisson earthquake occurrence assumption, the annual probability of exceeding a certain damage state can be finally calculated as follows:

$$P_{annual}(DS) = 1 - e^{-\lambda_{annual}(DS)} \tag{2-12}$$

The above exceedance probabilities of different seismic damage states can be easily converted into occurrence probabilities for no damage, slight, moderate, extensive, and complete as shown in Eq. (2-13), which then enable random sampling of bridge system-level damage states during any annual transition.

$$\mathbf{P_{occurrence}} = \begin{bmatrix} 1 - P_{annual}(slight) \\ P_{annual}(slight) - P_{annual}(moderate) \\ P_{annual}(moderate) - P_{annual}(extensive) \\ P_{annual}(extensive) - P_{annual}(complete) \\ P_{annual}(complete) \end{bmatrix} \tag{2-13}$$

2.5. Mapping from Seismic Damage States to Condition Ratings

The impact of seismic damage on the bridge conditions will be considered in this section. Here, a decision-tree based mapping is introduced to update the condition ratings of the three generic bridge components based on the system-level seismic damage states (i.e., the mapping from DS to CR shown in Figure 2-5). It is assumed here that the system-level seismic DS will affect the condition ratings for all the three bridge components. It is important to note that adjusting all three component condition ratings based on the bridge system-level seismic damage states will likely overestimate the seismic damage and risk, which is more conservative and acceptable compared to risk underestimation. Moreover, it is assumed that the maintenance actions will also cover the effect of seismic repairs, so that the AI-based decision agent to be mentioned in Chapter 4 can holistically offer decision support on regular maintenance as well as repairs after major earthquake events. The rationale behind merging the seismic repair actions into the maintenance actions is as follows: (1) From past literature [36–39], the direct costs and duration of seismic repair and maintenance actions are fairly similar as can be concluded from **Table 3-1**, **Table 3-3**, and **Table 3-6** in Chapter 3; (2) The AI decision agent in Chapter 4 may not be able to fully learn the underlying dynamics due to the relatively less frequent seismic repair actions, especially in those low/moderate-seismicity regions without sufficient training samples related to the effect of different intervention actions.

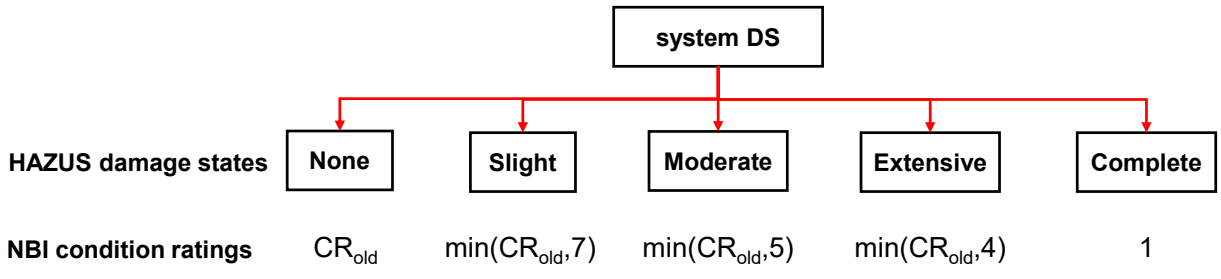

Figure 2-5. Mapping from system-level seismic damage states to component condition ratings

CHAPTER 3. RISK-BASED LIFE-CYCLE COST ANALYSIS

3.1. Introduction

Bridge infrastructure assets use significant investment in maintenance, retrofit, and replacement throughout their lifecycle. Transportation agencies, governments, and other stakeholders, seek to maximize the value of their investments in bridge asset management. As such, life-cycle cost analysis is an essential tool to evaluate the effectiveness and efficiency of bridge management programs. It provides decision-makers with the information necessary to make informed choices about resource allocation, project prioritization, and alternative plan comparison. By quantifying the costs associated with different bridge asset management strategies, stakeholders can identify opportunities to reduce costs, improve efficiency, and enhance the overall long-term performance and functionality of the bridge infrastructure.

Based on the integrated and stochastic bridge condition rating and seismic damage modeling environment in Chapter 2, Chapter 3 further maps these random bridge state estimates to monetary cost metrics considering the costs incurred due to multiple factors, including condition deterioration, maintenance, seismic damage, and seismic retrofitting in a life-cycle context. Also note that the uncertainties from the above sources will be propagated via random Monte-Carlo simulations by generating random samples of input variables and simulating the monetary cost, which will then serve as the reward signals in the AI-informed decision agent to be developed in Chapter 4. **Figure 3-1** shows an overview for annual cost quantification in this study, where the cost of a bridge is categorized into two parts: direct and indirect costs. Direct costs include the costs directly spent by the transportation agencies in maintenance and seismic retrofit actions taken during the planning horizon. Indirect costs are caused by the traffic carrying capacity reduction due to bridge condition deterioration, seismic damage, and maintenance actions. The annual costs are then aggregated by considering a discount factor to obtain the life-cycle cost estimates.

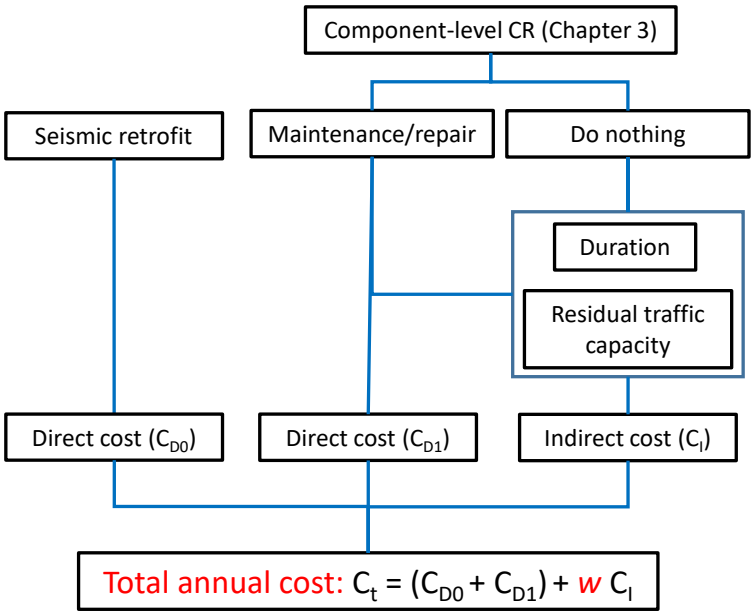

Figure 3-1. Workflow for annual cost estimation

3.2. Life-Cycle Direct and Indirect Cost Quantification

The direct and indirect costs, along with the total annual cost mentioned in **Error! Reference s ource not found.**, are all crucial cost measures. These measures provide essential reward signals for AI agent training. As noted in Chapter 4, the effectiveness of a maintenance policy is determined by its ability to minimize the life-cycle total cost.

3.2.1. Direct Cost

Direct costs in the management of existing bridges come from the costs associated with different intervention actions, particularly maintenance and seismic retrofit actions in the context of this research. The cost of the above intervention actions in bridge asset management can be commonly expressed in terms of a percentage of the total construction cost of the bridge components or the entire bridge.

3.2.1.1. Maintenance Costs

Maintenance costs can vary significantly depending on the type of maintenance actions. In this study, three types of maintenance actions are considered, including minor maintenance, major maintenance, and replacement for each of the three types of generic bridge components.

As shown in **Table 3-1**, the component-level maintenance direct costs are expressed as the percentage with respect to the total construction cost of the bridge components [27,36,40–42]. The total construction cost for deck, superstructure, and substructure is assumed to be 22.5%, 26.3% and 41.2% of the total bridge construction cost according to [36]. The total bridge construction cost is estimated as the product of the unit deck area cost and the total bridge deck area. In this study, the estimated unit deck area cost (in 2021 dollar values) is \$160.19/ft^2 of deck area for Tennessee, according to FHWA [43] after inflation adjustment [44].

Table 3-1. Maintenance cost ratio for different maintenance actions [27]

Maintenance action	Cost ratio (%)		
	Deck	Superstructure	Substructure
Do nothing	0	0	0
Minor	5	5	5
Major	25	25	25
Replacement	110	110	110

3.2.1.2. Seismic Retrofit Costs

Seismic retrofits improve the resistance of the bridges to seismic damage, and different retrofit actions can have different direct costs. Three seismic retrofit actions are considered herein, including steel jacketing (SJ) for bridge columns, seat extender (SE), and shear key (SK). The associated costs as a percentage of the total bridge construction cost are summarized in **Table 3-2** in which adopted from Huang et al. (2014) [45]. When more than one retrofit action is implemented, the direct cost for different retrofit actions is aggregated.

Table 3-2. Retrofit costs estimates

Retrofit action	SJ	SE	SK
Cost ratio (%)	12	3	3

For seismic repairs, as outlined in Section 2.5, the damage states are further mapped to condition ratings to reflect the impact of seismic damage, and maintenance actions are assumed to also cover the effect of seismic repair actions.

3.2.2. Indirect Cost

Apart from the direct costs related to intervention actions involved in bridge asset management, the indirect costs, which reflect the socioeconomic consequences due to the interruption to the bridges' traffic carrying capacity should be also considered. In this study, the indirect costs consist

of three parts: (1) vehicle operation cost; (2) time costs to passengers and trucks; and (3) safety cost. It is assumed that only maintenance actions will directly contribute to the indirect costs, as these intervention actions are recurrent and will result in traffic interruptions. The indirect costs incurred during the construction process of seismic retrofits are not considered due to the limited information related to the duration and level of traffic interruption of seismic retrofits. When more credible data is available, the related indirect costs can be easily incorporated. It should be noted that while the indirect costs during the retrofitting construction phase are not explicitly incorporated, the model still captures the long-term socioeconomic benefits of retrofitting, including enhanced resilience and reduced damage during seismic events.

Moreover, sensitivity analysis on several case study bridges with varying conditions showed that indirect costs from the retrofitting phase are relatively small compared to cumulative life-cycle costs due to deterioration and routine maintenance. Additionally, there is a lack of data in the literature on the durations and level of traffic interruptions for seismic retrofitting measures, making it challenging to accurately determine the indirect costs during the construction phase of seismic retrofits. The three retrofitting techniques (steel jacketing, seat extenders, and shear keys) also generally do not prolong bridge closures or traffic interruptions that would result in significant indirect costs during the retrofit construction phase.

3.2.2.1. Vehicle Operation Costs

The annual (365 days per year) vehicle operation cost, C_O, is computed as follows [46]:

$$C_O = \left[C_{O,car} \times (1 - r_{truck}) + C_{O,truck} \times r_{truck}\right] \times L \times ADT \times \left[\left(1 - \alpha_{sys} \times \phi_{sys}\right)T + \left(1 - \phi_{sys}\right) \times (365 - T)\right] \quad (3\text{-}1)$$

where ADT is the average daily traffic volume; $C_{O,car}$ and $C_{O,truck}$ are respectively the passenger car and truck operation cost rate; r_{truck} is the ratio of truck traffic; L is the detour length; T is the maximum duration (days) of the maintenance actions; and α_{sys} is the system-level residual traffic carrying capacity ratio during maintenance and can be determined according to **Table 3-3**. ϕ_{sys} denotes the traffic carrying capacity ratio related to bridge component condition deterioration

during normal operations and is determined based on the component-level ϕ factors as shown in Eqs. (3-2) to (3-5). Specifically, considering the bridge deck is in direct contact with the passing vehicles and typically receives the most maintenance actions and its condition has the most impact on the traffic carry capacity, it is assumed that ϕ_{deck} remains at 100% if the bridge deck condition rating is above or equal to 7 (i.e., within the FHWA "Good" conditions), then decreases linearly within the "Fair" conditions, and finally drops to zero once entering the "Poor" conditions, where the bridge is assumed to be closed due to safety concern until the bridge conditions are restored by proper intervention actions. For the ϕ factors for the superstructure and substructure, a simpler functional form is considered as shown in Eqs. (3-3) and (3-4), where the traffic carrying capacity remains at 100% for superstructure and substructure in "Good" and "Fair" conditions and drops to zero when reaching the "Poor" conditions. The bridge system-level residual traffic carrying capacity ϕ_{sys} is then dictated by the lowest component-level ϕ factor as shown in Eq. (3-5).

$$\phi_{deck} = \begin{cases} 1 & if\ CR_{deck} \geq 7 \\ 1 - \left(\frac{7 - CR_{deck}}{7}\right) \times 0.75 & if\ 4 < CR_{deck} < 7 \\ 0 & if\ CR_{deck} \leq 4 \end{cases} \quad (3\text{-}2)$$

$$\phi_{superstructure} = \begin{cases} 1 & if\ CR_{superstructure} \geq 5 \\ 0 & if\ CR_{superstructure} < 5 \end{cases} \quad (3\text{-}3)$$

$$\phi_{substructure} = \begin{cases} 1 & if\ CR_{substructure} \geq 5 \\ 0 & if\ CR_{substructure} < 5 \end{cases} \quad (3\text{-}4)$$

$$\phi_{sys} = min\{\phi_{deck}, \phi_{superstructure}, \phi_{substructure}\} \quad (3\text{-}5)$$

According to the past studies [36–39], the duration and residual traffic carrying capacity ratio corresponding to different maintenance actions are conjectured as listed in **Table 3-3**.

Table 3-3. Maintenance duration and residual traffic capacity

Action	Duration (days)	Residual traffic carrying capacity ratio (α_{sys})
Do nothing	0	1.00
Minor maintenance	3	0.75
Major maintenance	30	0.50
Rebuilding	182	0.00

3.2.2.2. Time Loss Costs

Additionally, the time loss costs due to traffic delay can be estimated as follows [46]:

$$C_T = \left[C_{W,car} \times O_{car} \times (1 - r_{truck}) + C_{W,truck} \times r_{truck}\right] \times ADT \times \frac{L}{V} \times \left[(1 - \alpha_{sys} \times \phi)T + (1 - \phi_{sys}) \times (365 - T)\right] \quad (3\text{-}6)$$

where $C_{W,car}$ is the hourly wage per passenger; O_{car} is the average occupancy per car; $C_{W,truck}$ is the hourly dollar value per truck; V is the average detour speed. These parameters are collected from the literature and are summarized in **Table 3-4**.

Table 3-4. Parameters for indirect cost estimation

Parameter	Description	Value (2021)	Ref.
$C_{O,car}$ **($/car/mile)**	Passenger car operation cost rate	0.64	[47]
$C_{O,truck}$ **($/truck/mile)**	Truck operation cost rate	1.855	[48]
$C_{W,car}$ **($/passenger/hr)**	Hourly wage per passenger	12.35	[44,49,50]
$C_{W,truck}$ **($/truck/hr)**	Hourly dollar value per truck	31.05	[44,49]
O_{car} **(number of passengers/car)**	Average occupancy per car	1.67	[50]
V **(mph)**	Average detour speed	50	[51]

3.2.2.3. Safety Cost

The cost of safety is not just about medical care and lost income; it also includes expenses related to pain, loss of comfort, and the wages of emergency staff. Wu et al. [52] conducted an analysis of the bridge during maintenance and presented the proportions of social cost components related to bridge maintenance. According to their findings, approximately 30% of the total indirect cost is linked to safety costs [52]. Consequently, indirect costs resulting from vehicle operation and time loss are increased in a way that results in 30% of the indirect costs being associated with safety (i.e., the sum of vehicle operation and time loss costs is multiplied by 1.43).

3.2.3. Total Cost

The above direct and indirect costs are then aggregated into the total annual cost. For the cost aggregation, a weighting factor w is introduced for the indirect costs as they are typically much higher than the direct costs. The aggregated total cost can be calculated based on Eq. (3-7)

$$C_{total} = (CD_0 + CD_1) + w \times (1 + \beta_s) \times (C_O + C_T) \quad (3\text{-}7)$$

where CD_0, and CD_1 respectively denote the direct cost due to seismic retrofit, and maintenance. w denotes the indirect cost weighting factor, which can be specified by the users to adjust the

indirect cost contribution to the total cost, and β_s represents the safety cost multiplier and is assumed to be 0.43 as discussed in Section 3.2.2.3.

3.2.4. Life-Cycle Cost Aggregation

The previous direct and indirect cost estimates are calculated only for a specific year, and should be aggregated to obtain the life-cycle cumulative costs to allow straightforward comparison of the long-term effect of different decision policies. The time-cumulative cost C_{TC} over a T-year planning horizon is calculated as follows:

$$C_{TC} = \sum_{t=1}^{T} \gamma^t C(t) \quad (3\text{-}8)$$

where $C(t)$ denotes the annual cost estimate at year t, $\gamma \in (0,1)$ is a factor accounting for the combined effect of inflation and discounting, and is considered to be 0.96 based on the USDOT Benefit-cost analysis guidance for discretionary grant programs [53].

3.3. Demonstrative Results

For demonstration purposes, a life-cycle cost analysis on a case-study bridge (as shown in **Table 3-5**), selected from the NBI database [18], is conducted to showcase the influence of different intervention actions on the bridge life-cycle costs. A 75-year planning horizon is considered, with 10,000 random life-cycle simulations (i.e., episodes) to incorporate the different sources of uncertainties. This assessment is performed by considering the bridge located in Memphis.

Table 3-5. Case study bridge specifications

Bridge parameter	Deck area (m^2)	Detour length (km)	Average Daily Traffic (Vehicle/day)	Truck ratio (r_{truck})
Value	809	19	14,740	0.02

Several prescribed intervention actions are considered as follows: 1) minor maintenance every 10 years; 2) major maintenance every 25 years; and 3) replacement at the 35th year, throughout the planning horizon (i.e., 75 years) of the bridge. In addition, a condition-based maintenance policy is also considered, with the following intervention actions triggering rules: do-nothing for components in the "Good" condition (CR = 7–9), minor maintenance for components in CR = 6, major maintenance for components in CR = 5, and replacement for components in the "Poor" condition (CR < 5). It should be noted that for all the above prescribed intervention actions, the

initial condition ratings for components are randomly sampled to be within the “Good” or “Fair” conditions (CR = 5–9).

3.3.1. Direct Cost Estimates

Figure 3-2 shows the average cumulative direct cost of the bridge over its lifetime (75 years) based on the 10,000 random episodes. As expected, performing minor maintenance every 10 years results in relatively low cumulative costs compared to the other maintenance actions; and replacing all three bridge components and the condition-based strategy are found to lead to higher cumulative direct costs. Since the initial condition ratings of the bridge components are randomly assigned, and the condition-based policy proposes both minor and major maintenance, direct costs associated with these maintenance activities may be incurred in the first year.

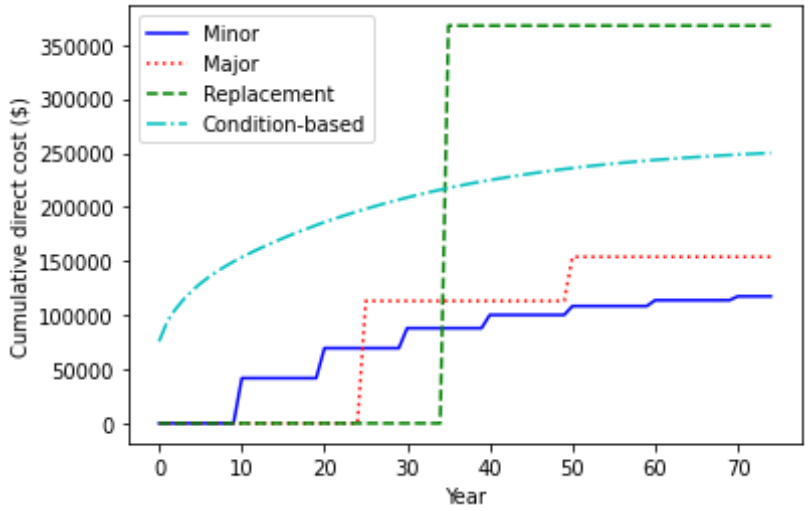

Figure 3-2. Average of cumulative direct cost of the bridge over a 75-year planning horizon

3.3.2. Indirect Cost Estimates

Figure 3-3 shows the expected absolute cumulative indirect cost during the 75-year time horizon. The condition-based maintenance policy leads to the lowest indirect cost, owing to the more active maintenance actions. Minor maintenance every 10 years results in the highest cumulative indirect cost due to their limited effectiveness in improving the condition ratings. Additionally, major maintenance actions every 25 years and replacing all three bridge components at the 35th year exhibit similar cumulative indirect costs over the bridge's lifetime.

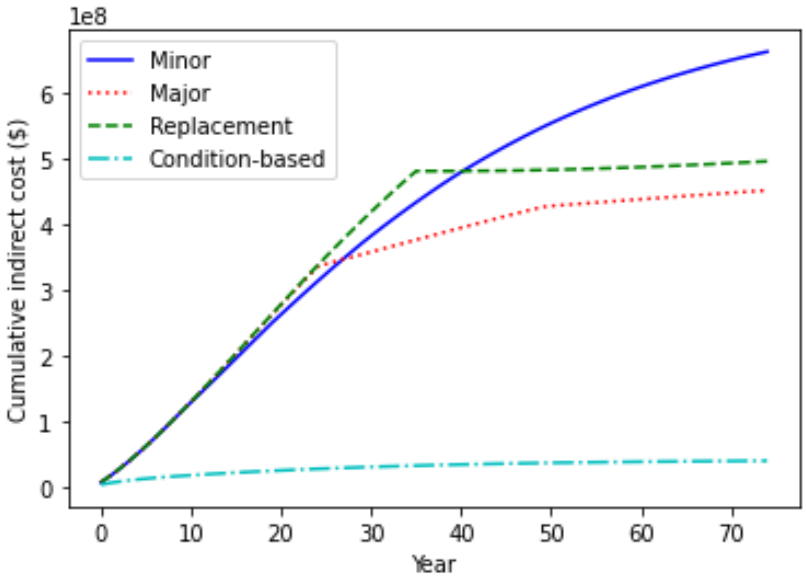

Figure 3-3. Average cumulative indirect cost of the bridge over a 75-year planning horizon

Furthermore, **Figure 3-4** shows the standard deviation of indirect cost over the bridge's lifetime for different intervention action strategies. It is noticeable that the standard deviation is lower for the condition-based policy due to the higher number of actions taken throughout the lifespan.

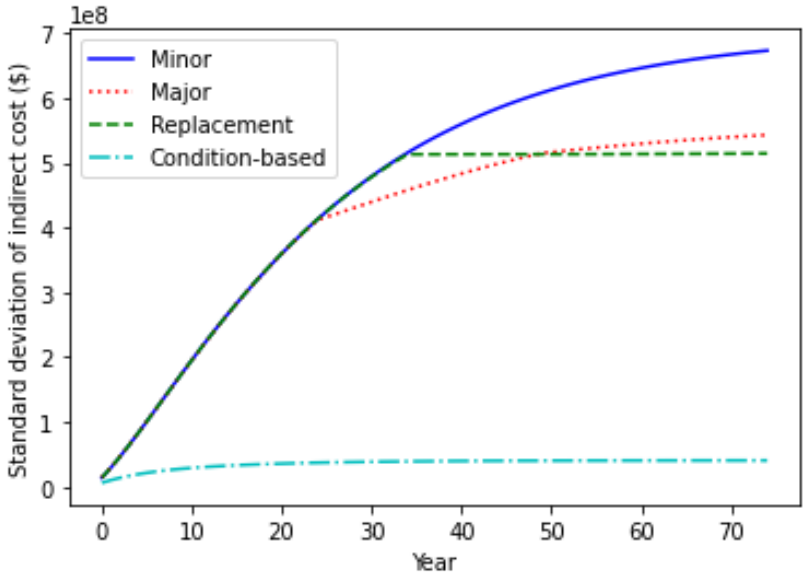

Figure 3-4. Standard deviation of cumulative indirect cost of the bridge over a 75-year planning horizon

3.3.3. Total Cost Estimates

In this section, the total life-cycle cost of the bridge after the weighted aggregation of the direct and indirect costs are examined. **Figure 3-5** shows the cumulative total cost by considering the indirect cost weight $w = 5\%$. The weighted indirect cost is introduced to prevent indirect costs from dominating the life cycle cost analysis. Overall, the cost module developed in Chapter 3 can holistically incorporate the direct and indirect costs incurred by multiple threats and intervention actions, and can offer quantitative life-cycle cost estimation and comparison of different maintenance strategies.

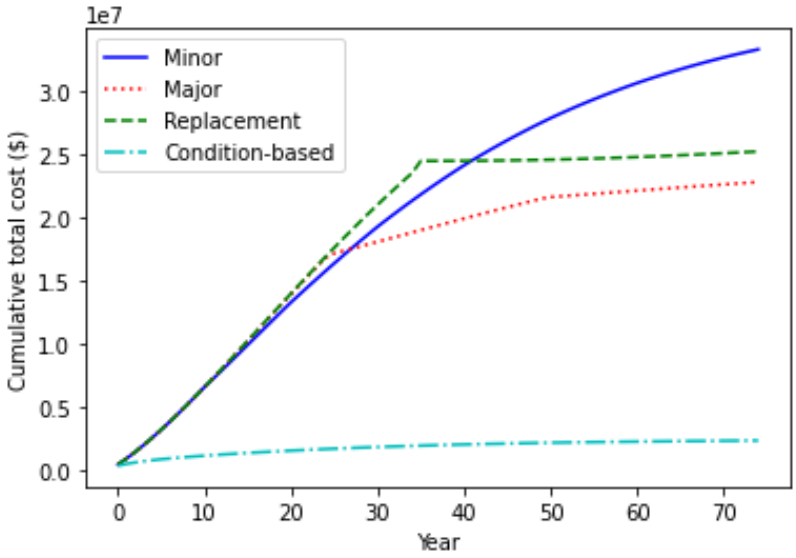

Figure 3-5. Average cumulative total cost curves of the case-study bridge over a 75-year planning horizon (w=5%)

3.3.4. Preliminary Benefit-Cost Analysis of Different Seismic Retrofit Strategies

This section presents a preliminary benefit-cost analysis to evaluate the effectiveness of various seismic retrofit strategies. Since the aging-induced condition deterioration, seismic damage, and intervention actions (i.e., maintenance and retrofit) all contribute to the direct and indirect costs, and these factors are highly intertwined, this simplified sensitivity analysis focuses exclusively on earthquake-related costs to assess the effectiveness of retrofit strategies. In other words, for all the analyses done within this subsection, the direct costs all stem from seismic repair activities, and

all the indirect costs are associated with the traffic interruption due to seismic damage and during seismic repair activities. More comprehensive benefit-cost analyses of seismic retrofit will be discussed in Section 4.5.5. To isolate the direct and indirect costs due to seismic damage, it is assumed here that there is no deterioration in bridge condition (i.e., CR = 9 all the time), and only seismic damage (without mapping to CR) can affect the traffic carrying capacities, and hence the indirect costs. It is assumed here that all seismic damage will be immediately repaired and the associated direct and indirect costs of seismic repairs are calculated based on the empirical repair cost, duration, and residual traffic carrying capacity estimates conjectured from past literature [36–39], as summarized in **Table 3-6**. As such, the direct costs include the retrofit costs as well as the seismic repair costs at the end of life of bridge, whereas the indirect costs only include the costs related to the reduction in traffic carrying capacity during the post-earthquake repair process. Again, a 75-year planning horizon is considered herein.

Table 3-6. Repair cost ratio, duration and residual traffic capacity

Damage state	Cost ratio (%)	Duration (days)	Residual traffic carrying capacity ratio (α)
Non	0	0	1.00
Slight	3	30	0.75
Moderate	8	130	0.50
Extensive	25	220	0.25
Complete	100	365	0.00

This evaluation is conducted for two different Cities (i.e., Memphis and San Francisco) with varying seismicity. In this analysis, the seismic fragility models remain the same as mentioned in Chapter 2 for both cities; only the seismic hazard curves differ. **Table 3-7** summarizes the results of the benefit-cost ratios (i.e., the reduced indirect cost compared to the no retrofit scenario versus the increased direct cost compared to the no retrofit scenario) for different retrofit strategies, where the retrofits are assumed to be implemented in the first year of the planning horizon. The benefit-cost ratio (BCR) is calculated as follows:

$$BCR = \frac{CI_{Noretro} - CI_{Retro}}{CD_{Retro} - CD_{Noretro}} \tag{3-9}$$

where $CI_{Noretro}$ and $CD_{Noretro}$ denote absolute life-cycle indirect cost and direct cost for cases without retrofitting and CI_{Retro} and CD_{Retro} denote absolute life-cycle indirect cost and direct cost for cases with seismic retrofitting.

As indicated in **Table 3-7**, the benefit-cost ratios vary across different retrofitting strategies and geographical locations with different seismicity. Between the two cities, it is observed that it is more cost-effective to implement seismic retrofit for San Francisco, which may experience more frequent earthquake events compared to Memphis.

Table 3-7. Benefit-cost ratio of different seismic retrofit strategies

Retrofit Strategies		No Retrofit	SJ	SE	SK	SE+SK	SJ+SE	SJ+SE+SK
Memphis	**CI ($)**	671,666	512,614	636,588	665,031	583,188	495,021	495,834
	CD ($)	8,495	174,076	49,317	50,184	90,459	215,547	257,345
	BCR	N/A	0.96	0.86	0.16	1.08	0.85	0.71
San Francisco	**CI ($)**	2,429,465	1,832,744	2,143,925	2,370,358	2,116,442	1,823,307	1,812,570
	CD ($)	31,443	191,846	67,586	72,007	108,590	232,863	274,526
	BCR	N/A	3.72	7.90	1.46	4.06	3.01	2.54

CHAPTER 4. AI-INFORMED BRIDGE-LEVEL SEQUENTIAL DECISION-SUPPORT

4.1. Introduction

According to the findings in NCHRP Synthesis 397 [54], the prevalent approaches for managing bridge assets tend to prioritize short-term over long-term benefits. These strategies lack resilience in dealing with uncertainty and do not adequately prepare for future risks. Moreover, the decision-making often centers narrowly on current agency expenses, overlooking the broader socio-economic consequences. Despite recent progress in incorporating life cycle planning and risk assessment into transportation asset management plans (TAMPs), these components still lack cohesive integration. For instance, risk evaluation remains predominantly qualitative, and systematic incorporation of quantitative risk analysis with life cycle planning is yet to be realized.

Recently, Reinforcement Learning (RL) has emerged as a promising approach for infrastructure management and maintenance planning. RL, a type of AI technique, learns the optimal sequential decision-making policy, by interacting with a stochastic and dynamic environment over time through trial-and-error. This mirrors how humans perceive and adapt to the real world. Recent studies have started exploring the potential of RL in supporting asset management and sequential decision-making for civil infrastructure systems [55–61]. Leveraging recent advancements in function approximators, particularly deep neural networks, Deep Reinforcement Learning (DRL) has emerged as a powerful approach to tackle RL challenges involving high-dimensional state and action spaces. Many of the aforementioned studies have also utilized DRL in their endeavors. However, past efforts primarily concentrated on individual structures rather than portfolios of structures, which could involve hundreds or even thousands of diverse structures. It is crucial to acknowledge that training dedicated AI decision models for each individual structure is both computationally demanding and labor-intensive. As such, the full potential of DRL's parameterization capabilities is yet to be exploited in the context of portfolio-level asset management. Moreover, past research mainly focused on chronic bridge condition deterioration, while the risks from other natural disasters (e.g., earthquakes) are yet to be integrated. This chapter aims to harness the potential of advanced AI techniques, specifically DRL, to provide

dynamic and risk-aware support for sequential maintenance decision making for a portfolio of highway bridges.

4.2. Methodology for AI-based Decision Support

In this chapter, fundamental concepts of RL and DRL will be first introduced, elaborating their relevance to the field of bridge maintenance and asset management. Next, detailed illustration of the proposed parameterized DRL for bridge asset management is provided.

4.2.1. Reinforcement Learning

RL has undergone remarkable progress in the past decade and has found wide application across various industrial and research domains, including robotics [62], autonomous vehicles [63], traffic signal control [64], and smart building energy management [65]. The bridge maintenance planning problem can be structured with a state space representing the conditions of individual bridge components; an action space encapsulates the possible intervention actions; state transition dynamics that govern how states can transition between each other under given actions; and reward functions indicating how effective are the actions when conditioned on different states. In this study, the bridge condition and seismic damage dynamics will be modeled based on the simulation environment in Chapter 2, and the life-cycle cost analysis in Chapter 3 will be used for reward quantification. The objective of RL is to derive an optimal policy for sequential decision-making to maximize the expected discounted cumulative reward, given the current bridge conditions.

In the context of RL, the AI agent, engages with the environment, which describes an individual bridge's deterioration dynamics, through a series of discrete time steps (e.g., years) denoted as "t". Assuming that the states of the environment are fully observable, during each time step, the agent receives the environment's states (e.g., conditions of bridge components), referred to as s_t, that belongs to the state space "S". The agent then makes a choice of action (e.g., maintenance actions), labeled as "a_t", from the action space "A". The execution of the chosen action then moves the environment to the next state ("s_{t+1}") based on the state-transition dynamics. In return, the agent receives an immediate reward ("r_{t+1}"), which is the total annual cost at that specific time step according to Eq. (3-7) in Chapter 3.

Over a given planning period of T time steps, a random interaction trajectory between the AI agent and the environment, from the beginning until the end of the planning period, is called an "episode", where the states, actions, and rewards in each time step are recorded. Because of the random nature of the environment, the main goal of RL training is to figure out the best decision policy, denoted as "$\pi(a_t|s_t)$", under different sources of uncertainties. This policy guides the selection of actions based on the current state of the environment, with the aim to maximize the expectation of the cumulative long-term reward ("R_t", as represented in Eq. (4-1)) throughout the planning horizon:

$$R_t = \sum_{i=t}^{t+T} \gamma^{i-t} r(s_i, a_i) \tag{4-1}$$

where: "γ" is a discount factor ranging between 0 and 1. A lower value of γ reduces the contribution of future rewards and vice versa. It is important to highlight that the equation for the long-term reward ("R_t") in Eq. (4-1) shares similarities with life-cycle cost quantification [66–68]. In this study, according to USDOT [53], a discount factor of 0.96 is considered to account for the combined effect of depreciation and inflation. Since the AI agent always tries to minimize the expected life-cycle total cost, which is a weighted summation the direct cost and indirect cost, it is thus also trying to reduce both direct and indirect costs. Intuitively speaking, this is equivalent to minimizing the traffic capacity reduction with the lowest maintenance cost.

4.2.2. Q-learning Algorithm

Q-learning [69] is a classic RL algorithm, as outlined in Eq. (4-2), to identify the best sequential decision-making policy, π. This policy guides the selection of actions that result in the highest expected cumulative reward over the long term, as represented by the Q values. In the Q-learning method, a Q table is used to store these Q values, each associated to a specific state-action pair. These Q values undergo iterative updates through the RL learning process, as depicted in Eq. (4-2), where "η" denotes the learning rate.

$$Q_{new}(s_t, a_t) \leftarrow Q_{old}(s_t, a_t) + \eta \left[r(s_t, a_t) + \gamma \max_{a \in A} Q_{old}(s_{t+1}, a) - Q_{old}(s_t, a_t) \right] \tag{4-2}$$

Here, the function "$Q(\cdot)$" is commonly referred to as the action-value function. "Q_{old}" and "Q_{new}" respectively correspond to the action-value function before and after each update. Q-

learning is an off-policy RL algorithm. This implies that during training, an alternative behavioral policy for action selection can be adopted, while the algorithm still ultimately converges toward the optimal action-value functions. Although Q-learning eventually achieves convergence even when employing a completely random behavioral policy during training, exploration-exploitation strategies like the ε-greedy method is commonly employed for better sample efficiency and faster convergence. The ε-greedy method seeks a balance between exploration (to uncover unvisited sequences) and exploitation (to leverage the already learned policy). Typically, for ε-greedy, the exploration probability initiates from a high value (e.g., 1.0) and gradually reduces as the training progresses. With a substantial number of training episodes, the Q values eventually reach convergence. In each time step, the action with the highest Q value is suggested.

4.2.3. Deep Reinforcement Learning

Q-learning trains the RL agent by iteratively updating the Q-values in each training step. However, this approach suffers from the curse of dimensionality, where the Q table's size can quickly blow up as the dimensions of the state and action spaces increase. Consequently, Q values' convergence can be remarkably slow, especially for problems with high dimensions. As such, DRL emerges as a robust approach by employing advanced function approximators like neural networks and decision trees, offering notable improvements in sample efficiency and convergence. Various DRL algorithms, such as Deep Q-Networks (DQN) [70], Deep Deterministic Policy Gradients (DDPG) [62], and Actor-Critic methods [71] have been developed. In the present study, the proposed DRL approach will be implemented by adapting a classic DRL algorithm, DQN, which employs neural networks to approximate the Q-values. DQN can also be implemented in conjunction with experience replay to improve the sample efficiency as well as to reduce the impact of correlation from sequential samples [70], by randomly sampling the past experience from a finite experience replay buffer. Here, each experience represents a one-step state-action transition. The experience replay buffer (D) has a maximum experience capacity and only the most recent transitions are stored. Finally, the policy neural network weights will be updated via common stochastic gradient descent algorithms in each training step. To facilitate more sample-efficient learning, prioritized experience replay (PER) [72], rather than the traditional random experience replay, is adopted. PER is a technique that prioritizes the replay of certain experiences in the agent's memory.

Traditional experience replay in reinforcement learning treats all experiences in the experience buffer with equal probability, which can lead to suboptimal learning. In prioritized experience replay DQN (PERDQN), experiences are assigned priorities based on their potential impact on learning, allowing the agent to focus more on important experiences.

4.2.4. Proposed Parameterized DQN Methodology for Maintenance Planning and Life-Cycle Risk Quantification for Highway Bridge Portfolios

Clearly, creating a dedicated DRL model for each bridge is impractical because of significant computational resources and development efforts. To deal with parameterized state or action spaces, where the environment is not constant but conditioned on certain parameters (e.g., the bridge attributes), a parameterized Deep Reinforcement Learning (P-DRL) approach is proposed herein for maintenance planning of various individual bridges within a bridge portfolio. In this setting, each bridge is represented by a unique environment with its own bridge-specific parameters. The pseudo codes of the proposed parameterized DQN algorithm with prioritized experience replay (P-PERDQN) are shown in **Table 4-1**.

Table 4-1. Parametrized DQN with prioritization pseudo code

Generate M random combinations of bridge-specific parameters $\{x_i\}$ via Latin Hypercube Sampling (LHS)
Specify minibatch k, step-size η, replay period for updating sample transition K and size N, exponents α and β, discount factor γ, planning horizon T
Initialize replay memory buffer $\mathcal{H}$, $\Delta = 0$, $p_1 = 1$
Initialize action-value function Q with random weights θ
Initialize target action-value function $\hat{Q}$ with weights $\theta^- = \theta$
For e = 1, M do
  Create a bridge-specific environment with one realization from the LHS bridge parameters x_i
  Observe s_0
  For t = 1, T do
    With probability select a random action a_t
    Otherwise select $a_t = argmax_a Q(s_t, a, x; \theta)$
    Observe s_t, r_t
    Store transition (s_t, a_t, s_{t-1}, r_t) in $\mathcal{H}$ with maximum priority $p_t = max_{i<t} p_i$
    If $t \equiv 0 \; mod \; K$ then
      For $j = 1$ to k do
        Sample transition $j \sim P(j) = p_j^\alpha / \sum_i p_i^\alpha$
        Compute importance-sampling weight $\omega_j = \left(N . P(j)\right)^{-\beta} / max_i \omega_i$
        Compute TD-error $\delta_j = R_j + \gamma_j Q_{target}\left(s_j, argmax_a Q(s_j, a, x)\right) - Q(s_{j-1}, a_{j-1}, x)$
        Update transition priority $p_j \leftarrow |\delta_j|$
        Accumulative weight-change $\Delta \leftarrow \Delta + \omega_j . \delta_j . \nabla_\theta Q(s_{j-1}, a_{j-1})$
      End for
      Update weights $\theta \leftarrow \theta + \eta . \Delta$, reset $\Delta = 0$
      From time-to-time copy weights into target network $\theta_{target} \leftarrow \theta$
    End if
  End for
End for

In this research, the P-PERDQN algorithm is developed by introducing the bridge-specific parameters as the model inputs. These parameters cover factors such as bridge deck area, average daily traffic volume, truck traffic ratio, and detour length, and data for these factors is widely available in the NBI database. The architecture of the neural network function approximator for the proposed P-PERDQN is shown in **Figure 4-1**. In this study, the neural network comprises two hidden layers, each containing 24 neurons. The "Adam" optimizer is employed to facilitate the training process, with an initial learning rate set to 0.01. This configuration aims to balance efficient learning with stability, ensuring the model converges effectively during training.

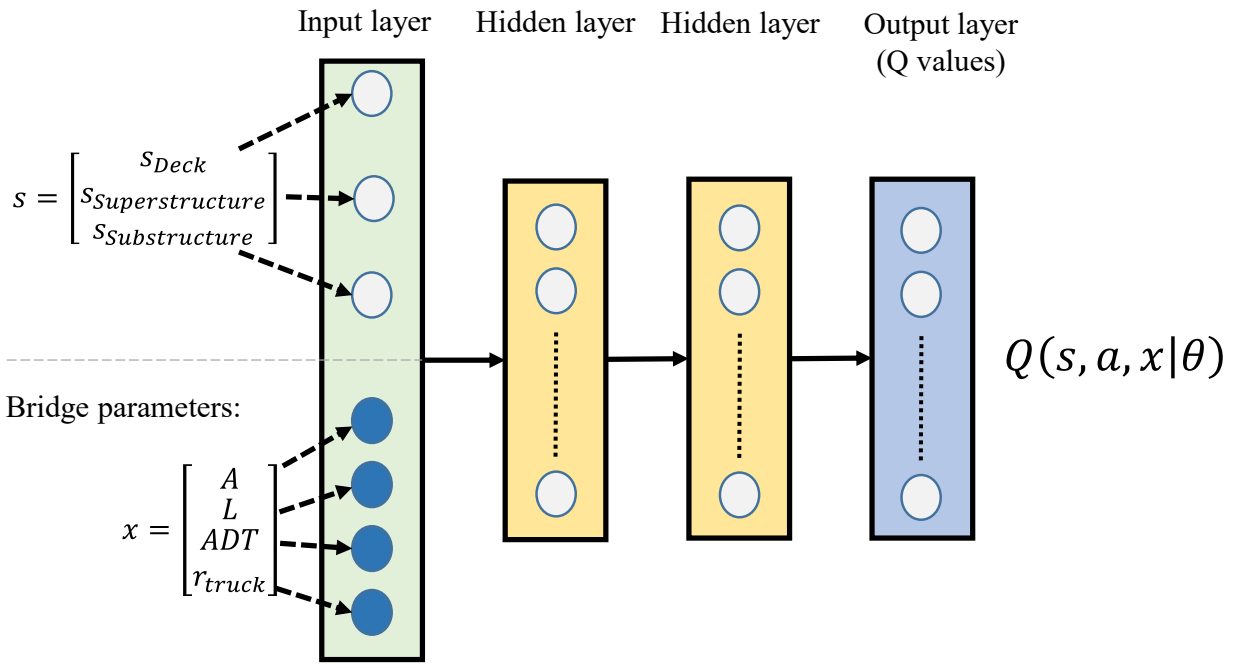

Figure 4-1. Architecture of the neural network function approximator for parameterized DQN

The key innovation, compared to traditional dedicated DRL algorithms for a specific individual bridge, is that the proposed approach can consider a distinct bridge environment in each training episode, and the Q functions are conditioned on the bridge-specific parameters. For each of these episodes, a random set of bridge-specific parameters are generated through the Latin Hypercube Sampling (LHS) [73]. LHS efficiently generates random samples of bridge-specific parameters covering the bridge parameter space. The bridge-specific parameters are introduced as additional inputs to the neural network function approximator, allowing the resulting P-PERDQN model to effectively accommodate the unique characteristics of various individual bridges.

Once the above parameterized DRL model is trained, it can be deployed to offer near real time sequential decision support for different bridges within a bridge portfolio. Moreover, the trained DRL model will be used to conduct Monte Carlo simulations for bridge life-cycle risk assessment. DRL's adaptive decision-making and risk assessment capabilities can facilitate more informed decision making in bridge asset management.

4.3. Traditional Condition-Based Maintenance Policies

To assess the efficacy of the AI-based decision methodology proposed in this study, a comparative study is carried out with other conventional condition-based policies (CBs) as follows:

CB-1: Do nothing for components in the "Good" conditions, do nothing for components in the "Fair" conditions, replacement for components in the "Poor" conditions.

CB-2: Do nothing for components in the "Good" conditions, minor maintenance for components in the "Fair" conditions, replacement for components in the "Poor" conditions.

CB-3: Do nothing for components in the "Good" conditions, minor maintenance for components with CR = 6, major maintenance for components with CR = 5, replacement for components in the "Poor" conditions.

4.4. Action Constrains for More Realistic Maintenance Policies

In order to ensure that the policies developed for bridge asset management comply with real-world practices, a set of practical constraints for training and testing of different policies are introduced to both the DRL-based and the condition-based approaches.

(1) Non-Consecutive Action Constraint: For any individual bridge, no consecutive actions are permitted on the same bridge component within a 5-year time frame, if the component condition rating is in the "Fair" or "Good" conditions. This constraint is not applied when the condition rating is "Poor". This constraint reflects the need for strategic planning and allocation of maintenance over time, ensuring that actions are temporally separated to optimize the use of resources and minimize disruption to the bridge's operation.

(2) Substructure Replacement Cascade: When a substructure replacement is executed, it triggers the complete reconstruction of the entire bridge. This constraint acknowledges the interconnected nature of bridge components and the significant impact that the replacement of a fundamental component can have on the entire bridge's structure and functionality.

(3) Girder Replacement Cascade: Similar to the previous constraint, the girder replacement cascade assumes that the replacement of bridge girders triggers the replacement of the bridge deck.

(4) Do Nothing for Good Condition Constraint: No action is permitted on a bridge component when its condition rating (CR) is within the "Good" condition (CR = 7–9). This constraint acknowledges that there is no need for maintenance actions on components that are already in excellent condition, preventing unnecessarily frequent interventions.

By incorporating the first three constraints into the training and all four constraints into the testing of bridge management policies, it is ensured that the resulting strategies are not only effective but also practical and aligned with the complexities of managing real-world bridge assets. Note that these action constraints can be modified when needed, and other user-specified practical constraints not listed here can also be incorporated.

4.5. Results

4.5.1. DRL-Based Policy Training

In the training process of the DRL models, 40,000 random episodes are employed to allow the AI agent to experience sufficient state transitions for different individual bridges. Note that the random bridge state transitions and reward signals are generated as outlined in Chapter 2 and 3, with both bridge condition deterioration and seismic damage risks considered. A 30-year planning horizon are considered as per [53], with a discount factor of 0.96 considered. In addition, a 5% indirect cost weight is considered to aggregate the direct and indirect costs into the total cost as discussed in Chapter 3, Eq. (3-7). The AI agent seeks to minimize the expected discounted cumulative total cost over the entire planning horizon. As a rule of thumb, the AI agent will less likely to perform maintenance actions with a lower indirect cost weight, and will be more actively performing maintenance actions with a higher indirect cost weight. It is suggested that the users experiment with this factor to achieve a desired balance between the direct and indirect costs.

Statistics of the case study bridge portfolio are provided in **Table 4-2**. In this table, uniformly distributed bridge parameters are considered to ensure that the random bridge realizations sufficiently cover the high-dimensional bridge feature space. This avoids bias towards any particular values and provides a fair representation of the entire parameter space. In addition, **Table 4-2** includes essential parameters that inform the DRL model training and testing. Furthermore, the initial conditions of the bridge components are initiated randomly to be within the "Fair" and

"Good" conditions, ensuring the model's adaptability to a wide range of real-world bridge current conditions. In this comparative study, two DRL-based methods are considered including the bridge dedicated DQN that can only be applied to a dedicated bridge, and the P-PERDQN that can accommodate different bridges within the entire bridge portfolio.

Table 4-2. Bridge portfolio parameters

Parameters	**Value [Range]**
Uniformly distributed random bridge parameters	
Deck area, A (m^2)	[100, 1200]
Detour distance, L (km)	[0.5, 20]
Average daily traffic, ADT (vehicles/day)	[500, 20,000]
Truck traffic ratio, r_{truck}	[0, 0.18]
Constant bridge parameters	
$C_{O,car}$ ($/car/mile)	0.64
$C_{O,truck}$ ($/truck/mile)	1.855
$C_{W,car}$ ($/passenger/hr)	12.35
$C_{W,truck}$ ($/truck/hr)	31.05
O_{car} (number of passengers/car)	1.67
Average detour speed, V (mph)	50
Bridge construction cost ($/$ft^2$ deck area)	160.19

Figure 4-2 shows the training curve for the portfolio-level DRL agent, P-PERDQN, incorporating three action constraints (cases 1, 2, and 3) outlined in Section 4.4 and without seismic retrofit. It is important to note that the fourth action constraint mentioned in Section 4.4 is not employed during the training process to the agent is allowed to learn as much knowledge as possible from the environment. As the training goes on, the agent's performance gradually improves until converging to the optimal policy. This stable and convergent curve is indicative of the DRL agent's ability to make effective decisions, minimizing the life-cycle total cost while maintaining a high level of stability.

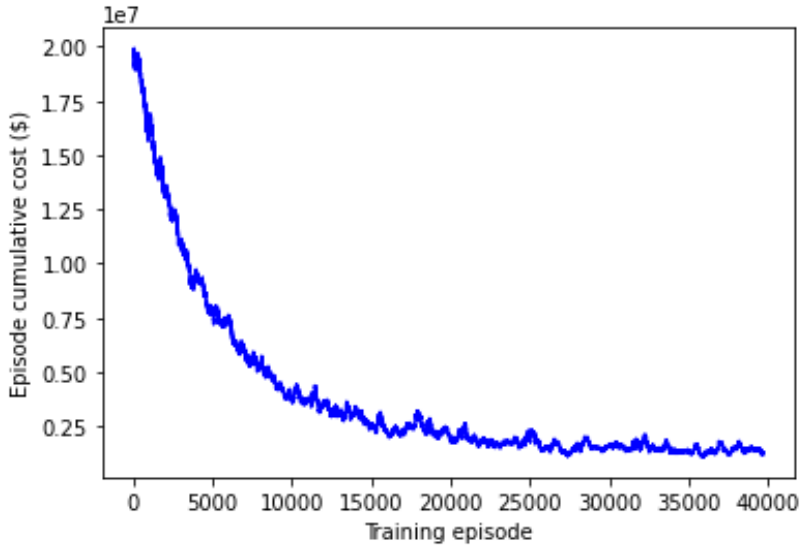

Figure 4-2. Training curve of the agent for DRL-based policies

4.5.2. Performance of the Portfolio-level DRL Agents on Individual Bridges

To evaluate how the portfolio-level DRL agent (P-PERDQN) performs on individual bridges, ten different individual bridges, covering a wide spectrum of the parameter ranges, are selected from the NBI database for Tennessee. Detailed information of the ten dedicated bridges is presented in **Table 4-3**.

Table 4-3. Parameters of the ten case-study individual bridges

Parameter	B1	B2	B3	B4	B5	B6	B7	B8	B9	B10
Deck area	200	407	606	899	1206	302	486	729	809	1009
ADT	6,000	3320	5860	1060	9240	690	2540	6440	14740	9540
L	1.0	8	2	8	16	8	8	3	19	2
r_{truck}	0.05	0.07	0.1	0.1	0.06	0.03	0.08	0.07	0.02	0.12

Figure 4-3 compares the average total cost incurred throughout the entire life cycle of the case study bridges by following different policies including portfolio-level DRL policy (P-PERDQN) and the dedicated DQN policy. This visualization underscores the superior performance of P-PERDQN compared to dedicated DQN, where P-PERDQN constantly delivers the lowest total costs for the case study bridges. Moreover, P-PERDQN also outperforms the dedicated DQN policy, with the advantage of more flexible applicability to different individual bridges without re-training the model.

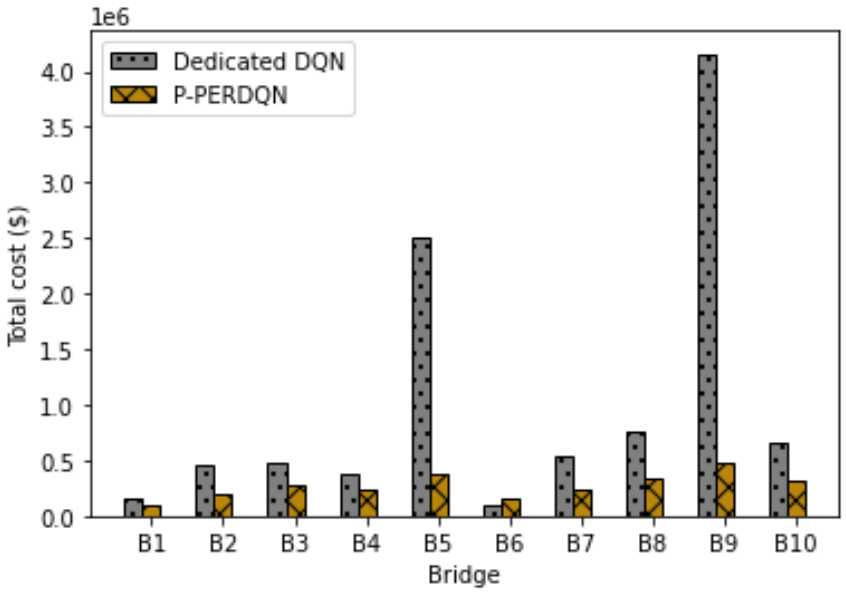

Figure 4-3. Total costs from different policies for case study bridges

4.5.3. Performance of the Portfolio-level DRL Agent on a Portfolio of Bridges

In this subsection, the portfolio-level DRL policy is assessed based on a bridge portfolio comprising 40,000 randomly generated bridges. Again, the initial CRs of the components for each bridge are randomly assigned to be within the "Fair" and "Good" conditions. **Figure 4-4** presents the average life-cycle direct, absolute indirect, and total (direct + weighted indirect) costs for a bridge within the case-study bridge portfolio. **Figure 4-4**(a) compares the average direct cost among the different policies, where P-PERDQN leads to the lowest direct cost compared to other condition-based policies. When it comes to indirect costs as shown in **Figure 4-4**(b), again it can be seen that the portfolio-level DRL policy (P-PERDQN) delivers comparatively much lower indirect costs to other condition-based policies. The above observations highlight the efficacy of P-PERDQN in minimizing not only the direct costs but also the indirect costs. **Figure 4-4**(c) presents the total cost for the portfolio-level comparison, again showcasing the superior performance of P-PERDQN among all the compared policies.

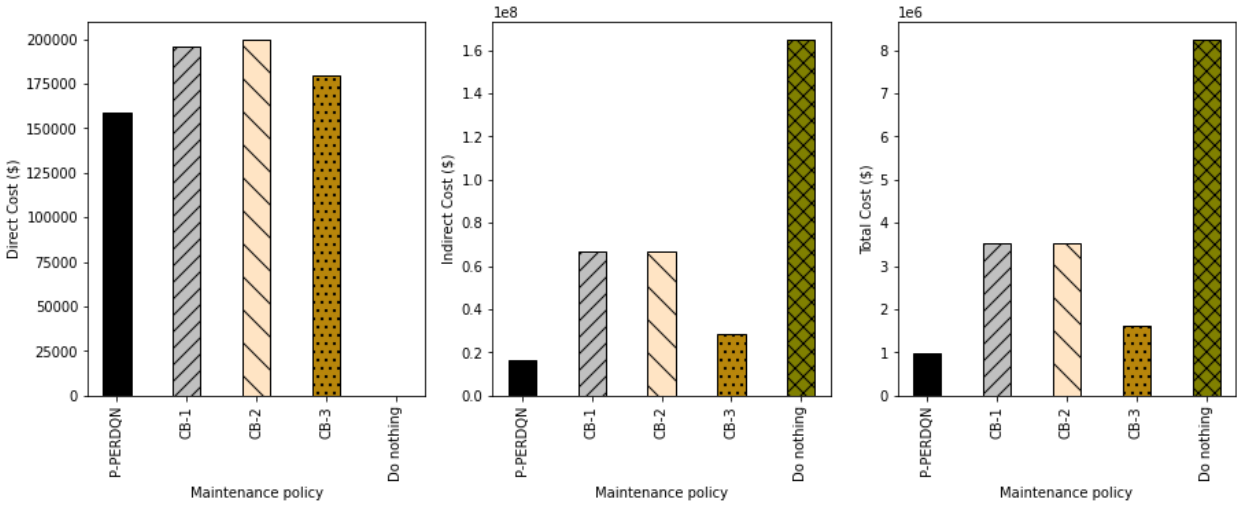

(a) (b) (c)

Figure 4-4. Life-cycle cost comparison of different bridge management policies on a portfolio of bridges: (a) Average direct cost, (b) Average indirect cost, (c) Average total cost

In addition, the condition ratings of three bridge components over the life cycle are compared for different maintenance policies. **Figure 4-5** shows the average condition ratings of the bridges at the portfolio level for various maintenance policies over the 40,000 random episodes. **Figure 4-5**(a) indicates that P-PERDQN maintains a higher condition rating (CR) compared to the three condition-based maintenance policies. Moreover, P-PERDQN is more active in preserving the deck condition to avoid the incurred indirect costs due to traffic carrying capacity reduction (see Eq. (3-2)). **Figure 4-5**(b) shows that P-PERDQN also maintains a higher CR for the superstructure compared to condition-based policies, while CB-3 provides a similar CR to P-PERDQN. **Figure 4-5**(c) demonstrates that CB-3 provides a higher CR for the substructure, while P-PERDQN keeps the CR close to that of the CB-3. The above result indicates that compared to the condition-based policies, P-PERDQN not only minimizes the life-cycle costs of the bridges but also effectively preserving the bridge conditions.

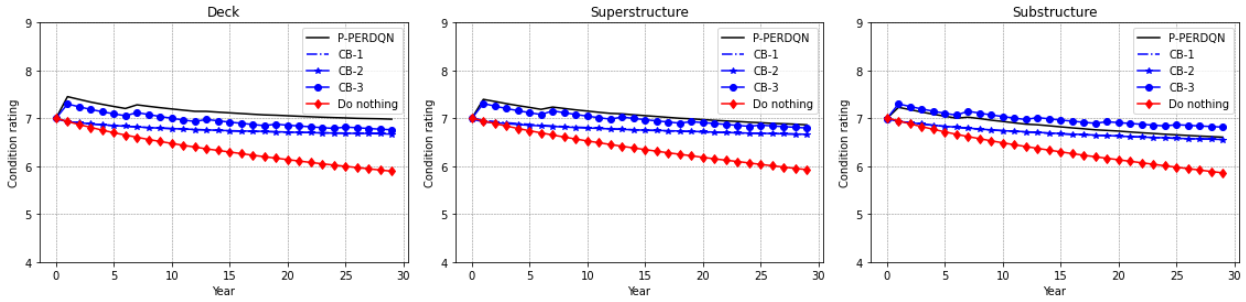

(a) (b) (c)

Figure 4-5. Average condition rating trajectories throughout the life cycle of the bridge portfolio: a) Deck, b) Superstructure, and c) Substructure

Furthermore, for a more comprehensive assessment of the life-cycle cost variability among different policies, Cumulative Distribution Functions (CDFs) of the life-cycle costs from the 40,000 random episodes compared. **Figure 4-6** shows the CDF for the average indirect cost, revealing that P-PERDQN results in a notably narrower spread of indirect cost distribution compared to other policies. This observation highlights the consistent and reliable performance of P-PERDQN, further emphasizing its effectiveness. Similar observations can also be found in **Figure 4-7**, which shows the CDFs of total cost across different policies, again showcasing the superior capability of P-PERDQN in effectively controlling the total life-cycle cost variability within a relatively low level.

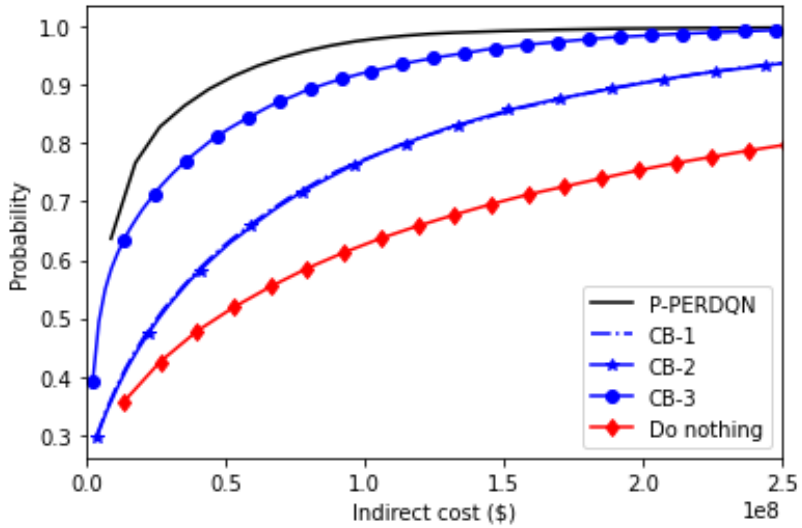

Figure 4-6. Comparison of indirect cost CDF among different decision policies

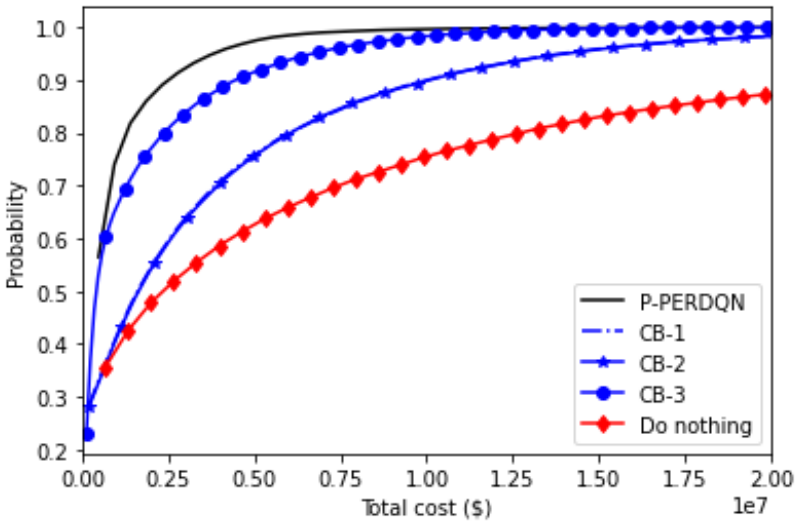

Figure 4-7. Comparison of total cost CDF among different decision policies

4.5.4. Toward More Transparent and Trustworthy AI-based Sequential Decision Making

When deploying the AI decision models, human decision makers (e.g., state DOT practitioners and engineers) may hope to understand the rationale behind the action suggestions from the AI agents. Moreover, it is also possible that the decision makers may need to override the suggestions by the AI agents due to other practical constraints, requirements, or personal judgement. Note that the AI agents merely offer action suggestions, it is up to the human decision makers to make the final decisions. In this regard, a decision visualization tool is developed to help the decision makers understand where different decisions stand among all the possible actions by comparing and visualizing the Q values, which measure the expected long-term benefit of different actions. Note that the Q values herein are of negative values as the DRL algorithms always strive to maximize the benefit (i.e., minimize the total costs). As such, the larger the Q values, the more effective are the actions.

In addition, following the readily trained P-PERDQN policy with the practical action constraints, some random episodic (i.e., life-cycle) condition rating and maintenance action trajectories are demonstrated on a case study bridges. Note that P-PERDQN is a portfolio-level policy that once trained, it can be applied to offer decision support for different individual bridges within a bridge portfolio.

For illustrative purposes, bridge B9 (see **Table 4-3**) is selected. **Figure 4-8**(a) demonstrates one random realization of condition trajectories for the three bridge components in the bridge's life timeframe and suggested actions by P-PERDQN. In addition, the 6^{th} year is selected for comparison purpose, when maintenance actions need to be determined. **Figure 4-8**(b) shows the Q values of the actions suggested by various policies along with the Q value range (the black line) of all the possible actions. The gray-filled bars in this figure represent the histogram of Q-values (i.e., occurrences or frequency of Q values within each bin) for the 64 action combinations, providing insights into the variability and spread of these values, which reflect the decision agent's assessment of the potential benefits of each action under the current bridge conditions. In addition, in this figure, the optimal action, the one with the highest Q value, is the one proposed by the P-PERDQN agent without considering the action constraints. The Q value for the action suggested by P-PERDQN with action constraints is close to the maximum Q value, and is slightly better than the condition-based policies. The implication from this particular example is twofold: (1) P-PERDQN is offering near optimal decisions; and (2) the condition-based policies are also reasonable alternatives, with very close Q values to those from the AI agents, if the decision-maker choose to override the AI decisions.

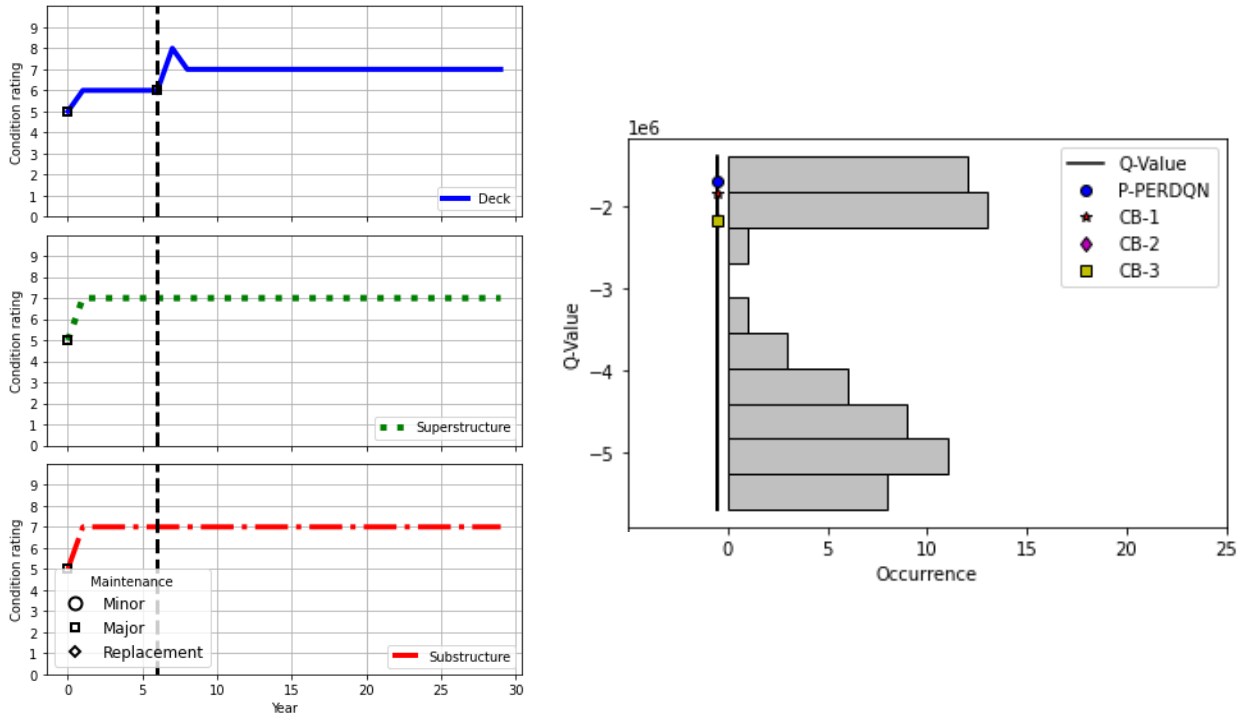

(a) (b)

Figure 4-8. One random realization without seismic damage for bridge B9: (a) Component condition rating trajectories, (b) Action Q values and the Q value range at 6th year

Figure 4-9 presents another random realization for the same bridge, where **Figure 4-9**(a) depicts one random realization of the three bridge components showing condition ratings and actions suggested by P-PERDQN. At the 11th year when an extensive damage occurred due to earthquake, the Q values of the suggested actions from various policies are compared in **Figure 4-9**(b). For this particular example, P-PERDQN performs the best with the highest Q value, whereas the three condition-based policies show inferior performance with much lower Q values compared with the AI-based policy.

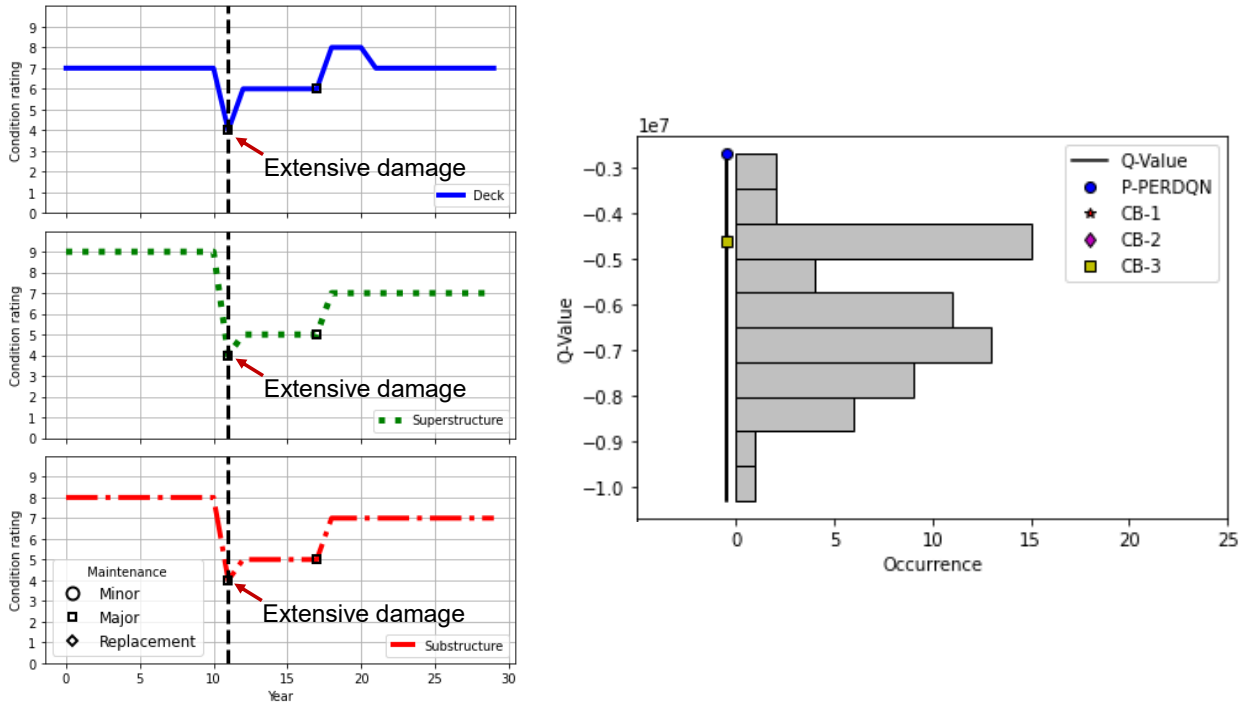

(a) (b)

Figure 4-9. One random realization with seismic damage for bridge B9: (a) Component condition rating trajectories, (b) Action Q values and the Q value range at 11th year

To examine the robustness of the AI-based policy (P-PERDQN) when mixed with other condition-based policies, a sensitivity study is carried out at the bridge portfolio-level to evaluate the effectiveness of combining P-PERDQN with CB-1 policy. The combined policy is termed as the Semi-DRL policy, with different mixing probabilities as shown in **Table 4-4**. In other words, at each decision time step, these mixing probabilities specify the probabilities of selecting the action from a specific decision policy (either the P-PERDQN or the CB-1). These Semi-DRL policies are considered to mimic the situation where the human decision-maker may sometimes override the AI suggestions.

Table 4-4. Mixing probabilities for the Semi-DRL policies

Policy	Semi-DRL-1	Semi-DRL-2	Semi-DRL-3	Semi-DRL-4	Semi-DRL-5
P-PERDQN	0.9	0.7	0.5	0.3	0.1
CB-1	0.1	0.3	0.5	0.7	0.9

The results for the average life-cycle costs of a bridge within the bridge portfolio are shown in **Figure 4-10** to compare the performance of the Semi-DRL policies, the pure DRL policy (P-PERDQN), and the pure condition-based policy (CB-1). As can be seen from the relatively consistent life-cycle costs for the first three Semi-DRL policies (Semi-DRL-1 to 3) compared to the pure DRL-based policy (P-PERDQN), when the DRL-based policy is dominant (i.e., with a selection probability ≥ 0.5), the AI-based policy is very robust with respect to random human override or interruption. As the probability of choosing the condition-based policy further increases beyond 0.5, the performance of the Semi-DRL policies quickly degrades with increasing life-cycle costs. Overall, from this sensitivity analysis, the AI-based policy is fairly robust with respect to human override.

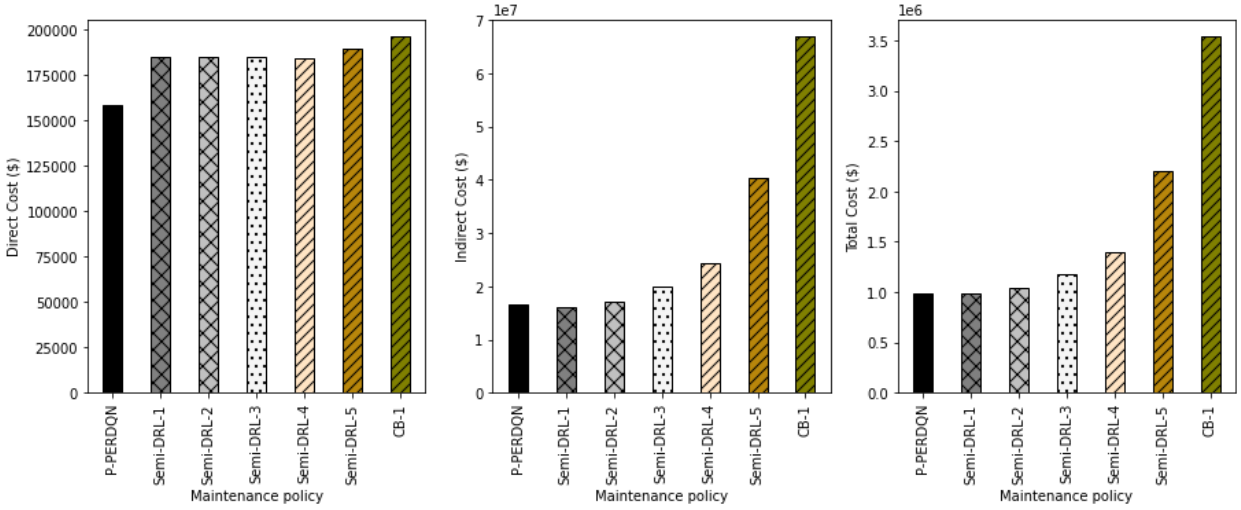

(a) (b) (c)

Figure 4-10. Comparison of life-cycle costs among different maintenance policies: (a) Direct cost, (b) Indirect cost, (c) Total cost

4.5.5. Comprehensive Benefit-Cost Analysis of Seismic Retrofitting

In this subsection, the influence of seismic retrofitting, when coupled with the AI-based maintenance policy, on the life-cycle costs is examined. Compared to the preliminary benefit-cost analysis in Section 3.3.4, the current study is more comprehensive by holistically integrating multiple intertwined factors, thereby offering more realistic evaluation of the effectiveness of seismic retrofitting. Particularly, the major difference from the preliminary benefit-cost analysis is

that now the time-evolving bridge condition ratings are incorporated without assuming that the condition ratings always stay at the best condition. Moreover, the AI decision agent is able to handle both maintenance action and seismic repairs, so that the assumption of immediate seismic repairs is dropped. Three scenarios are considered to train the AI-agents, with different environment settings: (1) condition deterioration only, (2) condition deterioration + seismic damage but no retrofitting, and (3) condition deterioration + seismic damage + multi-retrofitting. In the last scenario, multi-retrofitting refers to the combination of three retrofitting actions mentioned in Section 2.4.1 (i.e., steel jacketing + seat extender + shear key) implemented in the first year. Again, two cities (Memphis and San Francisco) with distinct seismicity are considered.

The average life-cycle direct and indirect costs are compared across different scenarios in **Figure 4-11** and **Figure 4-12** respectively for the two cities. Note that the direct costs include the cost due to seismic retrofit as well as the maintenance costs, while the indirect cost holistically incorporates the contributions from condition degradation, seismic damage, maintenance actions, and seismic retrofit. As expected, the results reveal that incorporating seismic hazard in the simulation environment increases the bridge life-cycle costs for both cities. This observation is particularly significant for San Francisco, given its higher frequency of earthquake occurrences compared to Memphis. Additionally, the benefits of the multi-retrofitting strategy (Scenario 3) can be observed through a reduction in indirect costs compared to Scenario 2 (without retrofit). Again, this benefit is more pronounced for San Francisco.

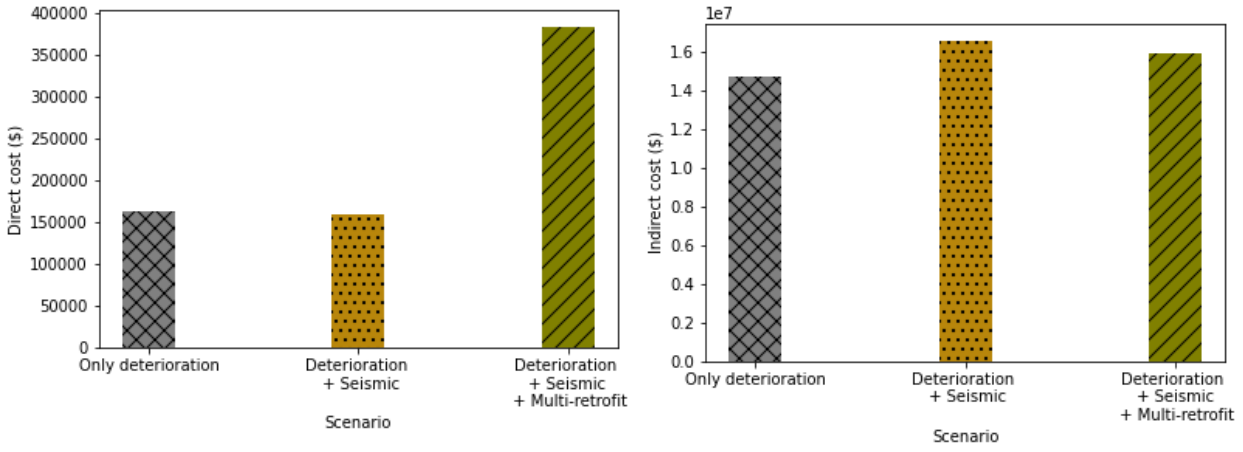

(a) (b)

Figure 4-11. Expected life-cycle costs of the AI-based policy under different environment settings for Memphis: (a) Direct cost, (b) Indirect cost

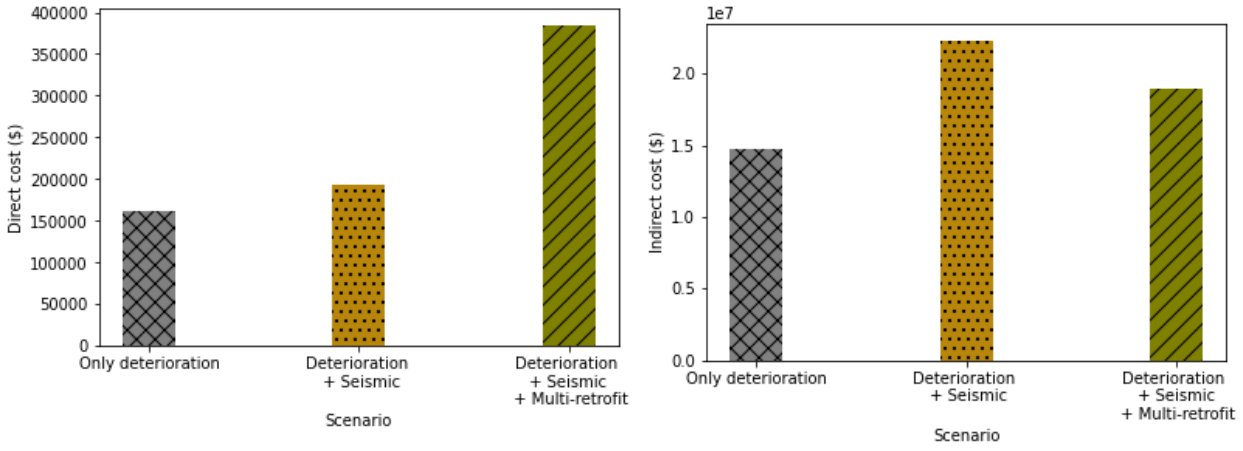

(a) (b)

Figure 4-12. Expected life-cycle costs of the AI-based policy under different environment settings for San Francisco: (a) Direct cost, (b) Indirect cost

Additionally, a benefit-cost analysis, based the ratio between the reduced absolute indirect costs versus the increased absolute direct costs as per Eq. (3-9), is carried out to examine the merit of seismic retrofit when coupled with the AI-based maintenance policy. In this investigation, both the absolute direct and indirect costs for Scenarios 2 (without retrofit) and 3 (with retrofit) are

utilized, and the resulting benefit-cost ratio can be interpreted as the ratio between the reduced indirect costs versus the increased direct costs. The results are presented in **Table 4-5**, which exhibits the same trend as discussed earlier in Section 3.3.4. The findings reveal that multi-retrofitting, when coupled with the AI-based maintenance policy, leads to a benefit-cost ratio greater than one, indicating tangible benefits. In simple terms, this ratio shows that the reduced life-cycle indirect cost is more than the increased direct cost. Thus, the investment in seismic retrofitting is justified based on this benefit-cost analysis. Furthermore, it is evident that the BCRs of seismic retrofit are more pronounced for San Francisco. And a longer planning horizon is found to further amplify the benefit of seismic retrofit as can be observed from the increasing BCR from a 30-year period to a 75-year period. Moreover, the BCRs when coupled with the AI-based maintenance policy are much higher compared to those from the preliminary benefit-cost analysis in Section 3.3.4, highlighting the importance of considering both maintenance strategies and seismic retrofit when conducting such life-cycle benefit-cost analysis.

Table 4-5. Benefit-cost ratio for multi-retrofit

City	**Planning Horizon**		
	30 years	75 years	
	Coupled with AI-based policy	Coupled with AI-based policy	Preliminary Analysis (Section 3.3.4)
Memphis	3.0	5.3	0.7
San Francisco	17.6	23.7	2.5

CHAPTER 5. CONCLUSION

This research developed an integrated and AI-based decision-support tool to better inform risk-aware and proactive sequential maintenance decision making for different individual bridges within a regional highway bridge portfolio. This tool consists of three major analysis modules including: 1) A multi-threat bridge degradation simulation environment that characterizes the stochastic and the condition transitions of bridge structures under chronic condition deterioration and seismic hazard threats, while also able to accommodate the effect of different maintenance and seismic retrofit actions; 2) A life-cycle cost analysis module quantifying and aggregating the direct and indirect costs due to bridge condition deterioration, seismic damage, and maintenance and retrofit actions over the planning horizon, and 3) An AI-informed decision-support module offering adaptive and proactive sequential maintenance suggestions over the life-cycle of different individual bridges within a regional bridge portfolio.

The bridge condition deterioration is modeled by considering bridge degradation due to aging deterioration and seismic hazard. Aging deterioration is characterized by using Markov chains, considering scenarios with no intervention (i.e., do-nothing) as well as various types of component-level maintenance actions. Additionally, bridge system-level seismic fragility models and seismic damage probability quantification are introduced to capture the effect of seismic hazard and seismic retrofit actions. Subsequently, the influence of seismic damage on bridge component condition ratings is addressed through a decision-tree-based approach, enabling updating of bridge component condition ratings based on the system-level seismic damage states.

Based on the above the integrated probabilistic simulation environment for bridge condition rating and seismic damage modeling, a life-cycle cost estimation module for direct and indirect costs incurred over the bridge's life cycle is established. These costs are evaluated annually and are then aggregated over the entire life cycle, factoring in discounting to adjust for depreciation and inflation. Furthermore, a preliminary benefit-cost analysis is conducted to assess the efficacy of various seismic retrofit strategies across different seismic hazard levels. Results reveal that it is more cost-effective to implement seismic retrofit for locations with higher level of seismicity.

By integrating the bridge simulation environment (Chapter 2) and the life-cycle cost quantification module (Chapter 3), a proactive AI-based decision-support tool was developed based on deep reinforcement learning (DRL) to offer sequential maintenance decision support for a portfolio of bridges. The proposed AI decision model is parametrized to accommodate the decision needs from various individual bridges within a bridge portfolio. The resulting portfolio-level DRL policy significantly reduces the computational burden of AI model training. Moreover, practical action constraints are introduced to align the proposed approach with real-world bridge management practices. These constraints help ensure that the developed policies are not only effective but also feasible and applicable in practical scenarios.

The portfolio-level DRL policies are first compared against bridge dedicated DRL policies in terms of the life-cycle management costs, highlighting the superior performance of the portfolio-level policy when applied to different individual bridges. At the bridge portfolio-level, the portfolio-level DRL policies also significantly outperform (in terms of the life-cycle costs) other traditional condition-based policies. Moreover, by visualizing the Q values of different alternative actions, an action visualization tool is developed to better help human decision makers understand the rationale behind the AI suggestions. To investigate the robustness of the DRL-based policy under potential human override, the DRL-based policy is mixed with a condition-based policy with different mixture probabilities. The results reveal that the AI-based policy is satisfactorily robust to potential human override. In addition, random episode realizations were presented to demonstrate the random life-cycle condition rating and maintenance action trajectories of select case study bridges, showcasing the dynamic and adaptable nature of the AI policies. Finally, a more comprehensive benefit-cost analysis is conducted to evaluate the effectiveness of seismic retrofitting when coupled with the AI-based policy.

In conclusion, the proposed AI-based sequential decision-making tool for bridge asset management can effectively integrate domain knowledge on probabilistic bridge condition degradation, seismic risks, and life-cycle cost estimation. This innovative tool can facilitate more proactive, adaptable, and long-term focused maintenance planning for a portfolio of bridges. By offering informed decision suggestions, it helps to significantly reduce the decision burden on

human decision makers, leading to more cost-effective bridge asset management and preservation of the nation's highway bridge infrastructure.

APPENDIX A. DEEP REINFORCEMENT LEARNING WITH PRIORITIZED EXPERIENCE REPLAY

Reinforcement Learning (RL) tracks and update the long-term benefit of different state-action pairs through the *Q* table (**Figure A-1**). However, maintaining the Q-table becomes impractical for high-dimension state- and action-spaces in many use cases. In this case, function approximators such as neural networks can be employed to estimate action values for any given state (**Figure A-2**). As such, Deep Reinforcement Learning (DRL) effectively combines the principles of RL with deep learning tools, and is more capable to deal with high-dimension problems.

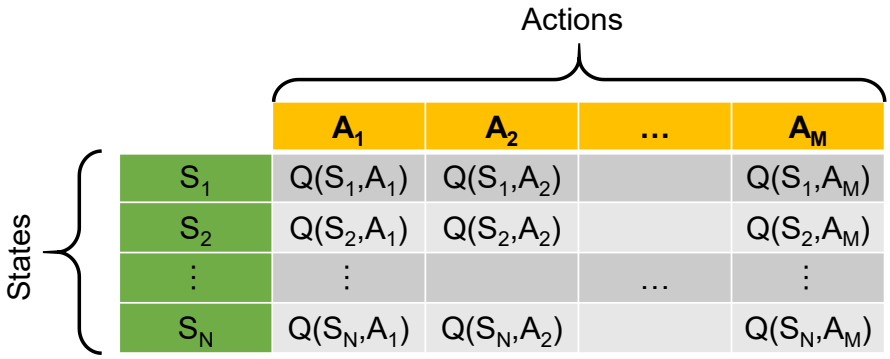

Figure A-1. Q learning

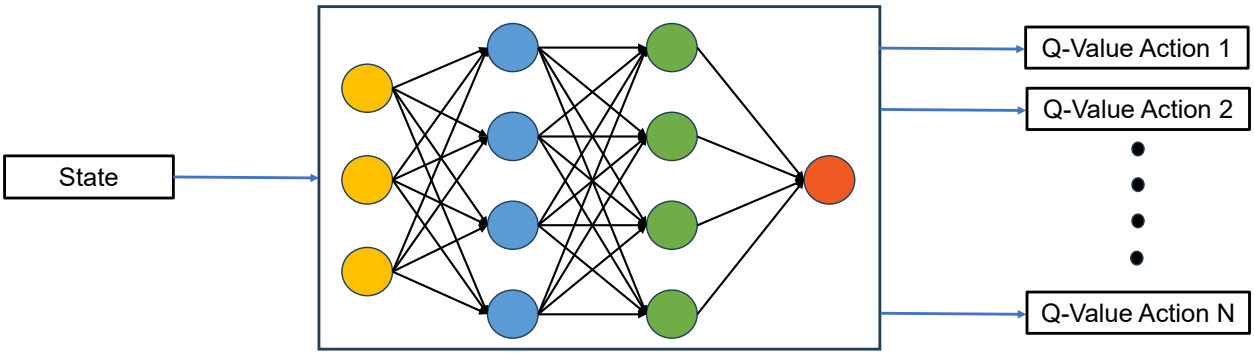

Figure A-2. Deep Q network learning

DQN, which stands for Deep Q-Network [70], builds upon the principles of *Q*-learning while incorporating additional elements such as a replay buffer and a target network, aimed at enhancing sample efficiency, policy learning stability and convergence. Initially, the replay buffer is empty,

and the weights of both the policy Q network and a separate target Q network are initialized at the beginning of the algorithm. The agent's state, S, is then initialized at the beginning of each episode.

Following the above setup phase, the optimization loop ensues, until convergence is achieved. During each iteration of this loop, an action is chosen based on the ε-greedy strategy, given the current state S_t. This action is executed within the environment, and the resulting new state along with the received reward are stored as a tuple in the replay buffer. For the policy Q network training, a minibatch of experiences are randomly sampled from the replay buffer, followed by a gradient descent step. Particularly, the loss function is computed against the target Q network $\hat{Q}_\theta$, which is updated less frequently compared to the policy Q network Q_θ. This approach facilitates the optimization process by providing a more stable policy training [74].

$$\mathcal{L}_t(\theta_t) = \mathbb{E}_{S_t, a_t \sim \rho(.)}\left[\left(\mathbb{E}_{S_{t+1}}\left(r + \gamma max_{a_{t+1}} \hat{Q}_{\theta_{t-1}}(s_{t+1}, a_{t+1}) \middle| s_t, a_t\right) - Q_{\theta_t}(s_t, a_t)\right)^2\right] \qquad \text{(A-1)}$$

$\rho(s_t, a_t)$ is the behavior distribution over S and a. Sampling the minibatch reduces the correlation that is inherent in reinforcement learning between subsequent states.

Another technique to facilitate more effective policy learning is called Prioritized Experience Replay (PER) [72]. In DQN, experience replay allows agents to reuse past examples. However, experiences are typically sampled uniformly, without considering their importance. The PER approach addresses this issue by prioritizing experiences. This means that important actions are replayed more often, thereby improving learning efficiency. The prioritization is based on the absolute temporal-difference (TD) error, a standard measure used in proportional prioritized replay.

The method of prioritizing transitions based solely on the greediness of TD errors encounters various challenges. Firstly, to avoid the computational burden of scanning the entire replay memory, TD errors are only updated for the transitions being replayed. This approach can lead to situations where transitions with initially low TD errors may not be revisited for a long time, or in some cases, may never be revisited at all, especially when using a sliding window replay memory. Additionally, this method is sensitive to sudden spikes in noise, such as when rewards are stochastic. Lastly, because greedy prioritization focuses on a small subset of experiences, the system may struggle with diversity, particularly when using function approximation.

To address these challenges, a stochastic sampling approach has been proposed that strikes a balance between pure greedy prioritization and uniform random sampling to ensure that the probability of being sampled increases monotonically with a transition's priority, while also guaranteeing a non-zero probability for even the lowest-priority transitions. In this regard, the sampling probability for transition *i* is as follows [72]:

$$P(i) = \frac{p_i^\alpha}{\sum_k p_k^\alpha} \tag{A-2}$$

where $p_i > 0$ is the priority of transition i. α is the prioritization level, with α = 0 corresponding to the uniform case.

Estimating the expected value with stochastic updates depends on these updates aligning with the same distribution as its expectation. However, prioritized replay introduces bias because it alters this distribution in an uncontrolled manner, thus affecting the solution that the estimates will converge to, even if the policy and state distribution remain constant. This bias can be corrected by employing importance-sampling (IS) weights as follows [72]:

$$w_i = \left(\frac{1}{N} . \frac{1}{P(i)}\right)^\beta \tag{A-3}$$

where N is the buffer size and β controls how much prioritization to apply.

APPENDIX B. KEY MODEL ASSUMPTIONS AND USER INPUTS

In this research, several assumptions, tentative values for some input parameters, and existing models from past literature were employed, many of which can be customized by the users or can be refined based on future research. These items are listed as follows and are elaborated subsequently:

Table B-1. Model assumptions and user inputs for bridge simulation environment setup

ID	Assumptions/User Inputs	Described in section(s)
1	State space (S)	2.3.1
2	Action space (A)	2.3.3
3	Number of components and their correlation	2.3.1 and 4.4
4	Markov state transition matrices ($\boldsymbol{P}$) for bridge components	2.3.2 and 2.3.3
5	System-level fragility models and seismic retrofit modification factors	2.4.1
6	Probabilistic seismic hazard curve	2.4.2
7	Seismic damage state (DS) to condition rating (CR) mapping	2.5
8	Initial condition ratings for bridge components	3.3

Table B-2. Model assumptions and user inputs for life cycle cost analysis

ID	Assumptions/User Inputs	Described in section(s)
1	Unit deck area cost	3.2.1.1
2	Cost ratio for maintenance and retrofit	3.2.1.1 and 3.2.1.2
3	Maintenance duration and residual traffic carrying capacity ratio (α)	3.2.2.1
4	Traffic carrying capacity ratio related to bridge component condition deterioration (ϕ)	3.2.2.1
5	Rates for passenger car operation ($C_{O,car}$) and truck operation ($C_{O,truck}$)	3.2.2.2
6	Hourly wage per passenger ($C_{W,car}$) and hourly dollar value per truck ($C_{W,truck}$)	3.2.2.2
7	Average occupancy per car (O_{car})	3.2.2.2
8	Average detour speed (V)	3.2.2.2
9	Indirect cost ratio contribution (w)	3.2.3 and 3.3.3
10	Discount factor (γ)	3.2.4
11	Repair duration and Residual traffic carrying capacity ratio (α)	3.3.4

Table B-3. Model assumptions and user inputs for the AI-based decision model

ID	Assumptions/User Inputs	Described in section(s)
1	Action constraints	4.4
2	Bridge portfolio parameters	4.5.1 and 4.5.2
3	DRL model hyper parameters	4.2.4, 4.5.1 and Appendix A
4	Planning horizon for bridge asset management (T)	3.3 and 4.2.1

Bridge Simulation Environment Setup (Chapter 2):

- *State space (S)*: In this study, bridge component condition ratings ranging from CR = 1 to CR = 9 are considered, as outlined in Section 2.3.1. Moreover, bridge-specific attributes including the average daily traffic volume, truck traffic ratio, detour length, and deck area are considered.
- *Action space (A)*: In this study, high-level actions such as "Do nothing," "Minor," "Major," and "Replacement" were considered for different bridge components, as outlined in Section 2.3.3. Note that the types of actions can be tailored according to user preferences.
- *Number of bridge components and their correlation*: In this study, bridge components such as "Deck," "Superstructure," and "Substructure" were considered. Some practical constraints are introduced to account for the dependencies among the bridge components. Specifically, replacement of substructures will trigger the replacement of the entire bridge, and replacement of superstructures will trigger deck replacement, as explained in Sections 2.3.1 and 4.4. It should be noted that the number of bridge components and their interdependencies can be adjusted by the users.
- *Markov state transition matrices (**P**) for bridge components*: In this study, the Markov transition matrices for the "do-nothing" action were derived based on the NBI data for Tennessee, and the Markov matrices for other maintenance actions are adapted from past studies, as outlined in Sections 2.3.2 and 2.3.3. Nevertheless, the users have the freedom to customize the Markov matrices.
- *System-level fragility models and seismic retrofit modification factors:* In this study, lognormal seismic fragility models as well as fragility model modification factor for seismic retrofit were adopted from past studies, as detailed in Section 2.4.1. The fragility models can be customized by the Users.
- *Probabilistic seismic hazard curve:* The USGS seismic hazard curves were adopted in this research as discussed in Section 2.4.2.
- *Seismic damage state (DS) to condition rating (CR) mapping*: In this study, a decision tree was employed to reflect the effect of damage states on bridge component condition ratings, as outlined in Section 2.5. This mapping can be adjusted by the users.

- *Initial condition rating for bridge components*: In this study, for the training of the AI decision models, initial bridge component condition ratings were randomly generated within the range from CR = 5 to CR = 9 (i.e., within the "Good" or "Fair" conditions), as detailed in Section 3.3. When deploying the trained AI policies on existing bridges, the actual bridge condition ratings, which are commonly documented in the NBI database, should be used.
- *Planning horizon for bridge asset management (T):* In this study, a 30-year planning horizon was considered for the AI decision model development, as discussed in Section 4.2.1. Users can specify the planning horizon based on the actual applications.

Life-cycle cost analysis (Chapter 3):

- *Unit deck area cost*: In this study, the unit deck area cost for Tennessee (adjusted to the 2021 dollar value) was obtained, as detailed in Section 3.2.1.1. The users should specify the unit deck area cost.
- *Cost ratio for maintenance and retrofit*: Component-level cost ratios for different intervention actions and retrofitting strategies can be customized by the users. In this study, these values derived as described in Sections 3.2.1.1 and 3.2.1.2.
- *Maintenance duration and residual traffic carrying capacity ratio (α)*: These values, used for the indirect cost calculations and can be redetermined by the user. In this study, these items are specified as outlined in Section 3.2.2.1 and **Table 3-3**.
- *Traffic carrying capacity ratio related to bridge component condition deterioration (ϕ)*: Traffic carrying capacity ratio of bridge based on the component's condition rating assumptions can be adjusted by the user. In this study, this ratio was based on the condition rating of deck, superstructure, and substructure, as discussed in Section 3.2.2.1.
- *Rates for passenger car operation* ($C_{O,car}$) *and truck operation* ($C_{O,truck}$): In this study, these values are specified in **Table 3-4**, and they can be customized by the users.
- *Hourly wage per passenger* ($C_{W,car}$) *and hourly dollar value per truck* ($C_{W,truck}$): In this study, these values are specified in **Table 3-4**, and they can be customized by the users.

- *Average occupancy per car (O_{car})*: In this study, this value is specified in **Table 3-4**, and it can be customized by the users.
- *Average detour speed (V)*: In this study, this value is specified in **Table 3-4**, and it can be customized by the users.
- *Indirect cost ratio contribution (w)*: A weighting factor can be adjusted to reflect a portion of indirect costs into the total life cycle cost based on stakeholder preference. In this study, a 5% contribution for indirect costs was considered, as shown in Sections 3.2.3 and 3.3.3.
- *Discount factor (γ)*: This factor accounts for inflation over the analysis cycle horizon. In this study, a compound discount factor of 0.96 was considered as outlined in Section 3.2.4.
- *Repair duration and Residual traffic carrying capacity ratio (α)*: These values used for a preliminary benefit-cost analysis and can be redetermined by the user. In this study, values were described in Section 3.3.4 and **Table 3-6**.

AI policy set up (Chapter 4):

- *Action constraints*: Practical constraints for training and testing policies were introduced to ensure compliance with real-world practices, and they can be customized by the users. In this study, the specific constraints were outlined in Section 4.4.
- *Bridge-specific attributes*: Bridge-specific attributes including deck area, average daily traffic, detour length, and truck ratio were introduced as inputs to the AI models. These bridge features are selected for their wide availability in the NBI database, although the users have the freedom to customize the bridge-specific parameters.
- *Bridge portfolio parameters*: Parameter ranges that reflect the variability of the bridge-specific attributes within a bridge portfolio along with other constants needed for cost estimation should be specified by the users. In this study, these parameters are specified in **Table 4-2**.
- *DRL model hyper parameters*: Users can adjust the DRL model hyperparameters such as the number of neurons, batch size, learning rate, and prioritization of samples as outlined in Sections 4.2.4, 4.5.1, and Appendix A.

APPENDIX C. COMPUTER CODES INSTRUCTIONS

This appendix provides the open-source Python codes for training and testing/deploying the AI decision agents. To achieve this, Github, a free web-based platform, is used to store the codes. In the following, a repository entitled "training-and-testing-deploying-the-AI-decision-agents" was created to store the developed codes:

https://github.com/AlirezaGhavidel70/training-and-testing-deploying-the-AI-decision-agents

To run the codes, with a Gmail account Google Colab can be used. In Google Colab, it is possible to run the codes either on your local computer or using the free cloud computing resources provided by Google.

To use a virtual machine, select the "Runtime > Change runtime type" option from the top menu bar in Colab. In the pop-up window, you can choose either CPU or GPU from the hardware acceleration options based on your preference. If you want to run the codes on your local computer, select the drop-down menu in the top-right corner of the code script (next to the small RAM and Disk performance charts).

Additionally, the web links for the codes are provided as follows:

1. **Training:** To train an AI-based agent model from scratch, use "Train_Agent"file in the shared Github repository. To use this file, simply click on the "Open in Colab".
   Then you can change the user inputs based on your preference as described in Appendix B. Otherwise, the agent will be trained based on the default inputs.
   To run this, simply select the "Runtime > Run all" option from the top menu bar in Colab. At the end of the web page, the training curve will be shown over episodes as described in Section 4.5.1. Once the training is completed, the trained model will be saved in your Google account, and you can access the saved model (trained model as a ". pth" file and the saved reward of each episode as a ".npy" file) through the left menu in Colab, located under "Files."
   Note: You can download a pre-trained model from the link provided (pre-trained AI model.pth) and use it for testing or deployment if you prefer not to train the AI agent

yourself. This model was trained using the data presented in this report and focuses on the case study in Memphis.

Testing/Deployment (suggested maintenance actions for a specific year): To view the suggested actions by the AI agent for a specific year, please use Colab file called "Annual_Decision". Then, if you want to test or deploy the readily trained AI agent, you just upload the "Trained_model.pth" file obtained from the training step.

To do this, once the Colab file is opened, run the first cell of the code and upload the provided "Trained_model.pth" file. In the user input section, enter the bridge parameters and the current condition rating of bridge components, including the deck, superstructure, and substructure. Note that the condition rating is between 1 and 9, as specified in **Error! Reference source not found.**. Finally, click on the second cell of the code and choose the "Runtime > Run after" option from the top menu bar in Colab. At the end of the Colab page, the suggested actions by the AI will be displayed based on your user inputs (bridge parameters and current condition rating of the bridge components).

2. **Testing/Deployment (random trajectory):** To test or deploy the available trained model and show a random trajectory of suggested actions and the condition rating of the three bridge components over time, use Colab file called "Random_Trajectory_Agent". Then, if you want to test the available trained model, you just upload the "Trained_model.pth" file. To do this, once you open the provided Colab link, upload the "Trained_model.pth" file by running the first cell of the code. Once the file is uploaded successfully, you can change some user inputs as described in Appendix B. Note that the bridge parameters for the testing phase should be within the same range as those the agent was trained on.

   Finally, simply click on the second cell and choose the "Runtime > Run after" option from the top menu bar in Colab. At the end of the web page, you will see the random realization plots. The results include the plots described in Sections 4.5.4.

3. **Testing/Deployment (life-cycle cost estimation):** To estimate the Life Cycle Cost, please use Colab file called "LCC_test_Agent". Then, if you want to test or deploy the readily trained AI agent, you just upload the "Trained_model.pth" file obtained from the training step.

To do this, once the Colab file is opened, run the first cell of the code and upload the provided “Trained_model.pth” file (or the saved model from training code in shared file #1). In the user input section, you can choose to test the model on the dedicated bridge (the bridge parameters can also be entered by the user) or on a portfolio of bridges (the range of the portfolio should be the same as the range of values where the model was trained in shared file #1). Finally, click on the second cell of the code and choose the “Runtime > Run after” option from the top menu bar in Colab.

At the end of the Colab page, statistical parameters (standard deviation and mean) are reported for total cost, direct cost, and indirect cost as described in Sections 4.5.2 and 4.5.3.

REFERENCES

[1] ASCE 2021 *Infrastructure Report Card*

[2] Liu H and Zhang Y 2020 Bridge condition rating data modeling using deep learning algorithm *Structure and Infrastructure Engineering* **16** 1447–60

[3] Assaad R and El-adaway I H 2020 Bridge infrastructure asset management system: Comparative computational machine learning approach for evaluating and predicting deck deterioration conditions *Journal of Infrastructure Systems* **26** 04020032

[4] Jiang Y, Saito M and Sinha K C 1988 Bridge performance prediction model using the Markov chain *TRB* 1180 (Transportation Research Board)

[5] Morcous G 2006 Performance prediction of bridge deck systems using Markov chains *Journal of performance of Constructed Facilities* **20** 146–55

[6] Yang D Y and Frangopol D M 2018 Risk-informed bridge ranking at project and network levels *Journal of Infrastructure Systems* **24** 04018018

[7] Thompson P D, Small E P, Johnson M and Marshall A R 1998 The Pontis bridge management system *Structural engineering international* **8** 303–8

[8] Johnson J and Boyle Z 2017 Implementation of AASHTOWare Bridge Management 5.2. 3 to meet agency policies and objectives for bridge management and address FHWA requirements *Eleventh International Bridge and Structures Management Conference* p 188

[9] Choi E, DesRoches R and Nielson B 2004 Seismic fragility of typical bridges in moderate seismic zones *Engineering structures* **26** 187–99

[10] Nielson B G and DesRoches R 2007 Analytical seismic fragility curves for typical bridges in the central and southeastern United States *Earthquake spectra* **23** 615–33

[11] Padgett J E and DesRoches R 2008 Methodology for the development of analytical fragility curves for retrofitted bridges *Earthquake Engineering & Structural Dynamics* **37** 1157–74

[12] Du A and Padgett J E 2020 Investigation of multivariate seismic surrogate demand modeling for multi-response structural systems *Engineering Structures* **207** 110210

[13] Du A, Cai J and Li S 2021 Metamodel-based state-dependent fragility modeling for Markovian sequential seismic damage assessment *Engineering Structures* **243** 112644

[14] Ghosh J and Padgett J E 2010 Aging considerations in the development of time-dependent seismic fragility curves *Journal of Structural Engineering* **136** 1497–511

[15] Ghosh J and Sood P 2016 Consideration of time-evolving capacity distributions and improved degradation models for seismic fragility assessment of aging highway bridges *Reliability Engineering & System Safety* **154** 197–218

[16] Simon J, Bracci J M and Gardoni P 2010 Seismic response and fragility of deteriorated reinforced concrete bridges *Journal of Structural Engineering* **136** 1273–81

[17] FEMA 2013 *HAZUS-MH 2.1 Earthquake Model Technical Manual* (Washington, D.C)

[18] FHWA 2022 National Bridge Inventory Data

[19] Agrawal A K, Kawaguchi A and Chen Z 2010 Deterioration rates of typical bridge elements in New York *Journal of Bridge Engineering* **15** 419–29

[20] Hatami A and Morcous G 2012 Deterioration models for life-cycle cost analysis of bridge decks in Nebraska *Transportation research record* **2313** 3–11

[21] Moomen M, Qiao Y, Agbelie B R, Labi S and Sinha K C 2016 *Bridge deterioration models to support Indiana's bridge management system* (Joint Transportation Research Program)

[22] Shen Y, Goodall J L and Chase S B 2019 Condition State–Based Civil Infrastructure Deterioration Model on a Structure System Level *Journal of Infrastructure Systems* **25** 04018042

[23] FHWA 2018 Bridge Preservation Guide: Maintaining a Resilient Infrastructure to Preserve Mobility

[24] Wang F, Lee C-C "Barry" and Gharaibeh N G 2022 Network-level bridge deterioration prediction models that consider the effect of maintenance and rehabilitation *Journal of Infrastructure Systems* **28** 05021009

[25] Thompson P D and Shepard R W 1993 Pontis *7TH CONFERENCE ON BRIDGE MANAGEMENT-PREPRINTS*

[26] Arif F, Bayraktar M E and Chowdhury A G 2016 Decision support framework for infrastructure maintenance investment decision making *Journal of Management in Engineering* **32** 04015030

[27] California Department of Transportation 2021 Transportation Asset Management Plans

[28] Tennessee Department of Transportation 2019 Transportation Asset Management Plans

[29] Texas Department of Transportation 2020 Transportation Asset Management Plans

[30] Johnston D W, Hooks J M, Welch E S, Marshall A R and Shaffer J K 2014 *Practical Bridge Preservation Actions and Investment Strategies* (National cooperative highway research program (NCHRP))

[31] FHWA 2022 *Specifications for the national bridge inventory* (Federal Highway Administration Washington, DC, USA)

[32] Padgett J E, Dennemann K and Ghosh J 2010 Risk-based seismic life-cycle cost–benefit (LCC-B) analysis for bridge retrofit assessment *Structural safety* **32** 165–73

[33] Field E H, Jordan T H and Cornell C A 2003 OpenSHA: A developing community-modeling environment for seismic hazard analysis *Seismological Research Letters* **74** 406–19

[34] Silva V, Crowley H, Pagani M, Monelli D and Pinho R 2014 Development of the OpenQuake engine, the Global Earthquake Model's open-source software for seismic risk assessment *Natural Hazards* **72** 1409–27

[35] Bradley B A, Dhakal R P, Cubrinovski M, Mander J B and MacRae G A 2007 Improved seismic hazard model with application to probabilistic seismic demand analysis *Earthquake engineering & structural dynamics* **36** 2211–25

[36] Elbehairy H 2007 *Bridge management system with integrated life cycle cost optimization* (University of Waterloo)

[37] Karamlou A and Bocchini P 2017 Functionality-fragility surfaces *Earthquake engineering & structural dynamics* **46** 1687–709

[38] Chang L, Peng F, Ouyang Y, Elnashai A S and Spencer Jr B F 2012 Bridge seismic retrofit program planning to maximize postearthquake transportation network capacity *Journal of Infrastructure Systems* **18** 75–88

[39] Mackie K R and Stojadinović B 2005 *Fragility basis for California highway overpass bridge seismic decision making* (Pacific Earthquake Engineering Research Center, College of Engineering …)

[40] Sun X, Zhang Z, Wang R, Wang X and Chapman J 2004 Analysis of past national bridge inventory ratings for predicting bridge system preservation needs *Transportation research record* **1866** 36–43

[41] Testa R B and Yanev B S 2002 Bridge maintenance level assessment *Computer-Aided Civil and Infrastructure Engineering* **17** 358–67

[42] Liu M and Frangopol D M 2005 Balancing connectivity of deteriorating bridge networks and long-term maintenance cost through optimization *Journal of Bridge Engineering* **10** 468–81

[43] FHWA 2021 Bridge replacement unit costs

[44] Labor U D 2021 US Bureau of Labor Statistics *Retrieved from*

[45] Huang Y, Parmelee S and Pang W 2014 Optimal retrofit scheme for highway network under seismic hazards *International Journal of Transportation Science and Technology* **3** 109–28

[46] Du A and Ghavidel A 2022 Parameterized deep reinforcement learning-enabled maintenance decision-support and life-cycle risk assessment for highway bridge portfolios *Structural Safety* **97** 102221

[47] Anon 2021 *Driving costs* (AAA Auto Insurance)

[48] ATRI 2021 *ATRI's newest operational costs research documents costliest year ever in trucking* (American Transportation Research Institute)

[49] FHWA 2021 *Work zone road user costs- Concepts and applications*

[50] FHWA 2017 *Summary of travel trends*

[51] Saydam D, Frangopol D M and Dong Y 2013 Assessment of risk using bridge element condition ratings *Journal of Infrastructure Systems* **19** 252–65

[52] Wu K, Yang D Y, Frangopol D M and Jin W 2021 Multi-stakeholder framework for assessing the life-cycle social cost of construction projects *Structure and Infrastructure Engineering* **18** 129–44

[53] USDOT 2018 *Benefit-cost analysis guidance for discretionary grant programs* (USDOT Washington, DC)

[54] Markow M J and Hyman W A 2009 *Bridge management systems for transportation agency decision making* vol 397 (Transportation Research Board)

[55] Wei S, Bao Y and Li H 2020 Optimal policy for structure maintenance: A deep reinforcement learning framework *Structural Safety* **83** 101906

[56] Memarzadeh M and Pozzi M 2019 Model-free reinforcement learning with model-based safe exploration: Optimizing adaptive recovery process of infrastructure systems *Structural Safety* **80** 46–55

[57] Tao W, Lin P and Wang N 2021 Optimum life-cycle maintenance strategies of deteriorating highway bridges subject to seismic hazard by a hybrid Markov decision process model *Structural Safety* **89** 102042

[58] Zhang Y and Burton H V 2021 Optimal decision-making for tall buildings in the aftershock environment *Automation in Construction* **122** 103472

[59] Andriotis C P and Papakonstantinou K G 2019 Managing engineering systems with large state and action spaces through deep reinforcement learning *Reliability Engineering & System Safety* **191** 106483

[60] Sun J and Zhang Z 2020 A post-disaster resource allocation framework for improving resilience of interdependent infrastructure networks *Transportation Research Part D: Transport and Environment* **85** 102455

[61] Du A and Ghavidel A 2022 Deep reinforcement learning enabled life-cycle seismic ris k assessment considering sequential seismic hazard and intervention actions *12th Natl. Conf. Earthq. Eng*

[62] Lillicrap T P, Hunt J J, Pritzel A, Heess N, Erez T, Tassa Y, Silver D and Wierstra D 2015 Continuous control with deep reinforcement learning *arXiv preprint arXiv:1509.02971*

[63] Kiran B R, Sobh I, Talpaert V, Mannion P, Al Sallab A A, Yogamani S and Pérez P 2021 Deep reinforcement learning for autonomous driving: A survey *IEEE Transactions on Intelligent Transportation Systems* **23** 4909–26

[64] Chu T, Wang J, Codecà L and Li Z 2019 Multi-agent deep reinforcement learning for large-scale traffic signal control *IEEE Transactions on Intelligent Transportation Systems* **21** 1086–95

[65] Yu L, Qin S, Zhang M, Shen C, Jiang T and Guan X 2021 A review of deep reinforcement learning for smart building energy management *IEEE Internet of Things Journal* **8** 12046–63

[66] Kumar R, Gardoni P and Sanchez-Silva M 2009 Effect of cumulative seismic damage and corrosion on the life-cycle cost of reinforced concrete bridges *Earthquake Engineering & Structural Dynamics* **38** 887–905

[67] Dong Y and Frangopol D M 2016 Probabilistic time-dependent multihazard life-cycle assessment and resilience of bridges considering climate change *Journal of Performance of Constructed Facilities* **30** 04016034

[68] Padgett J E and Tapia C 2013 Sustainability of natural hazard risk mitigation: Life cycle analysis of environmental indicators for bridge infrastructure *Journal of Infrastructure systems* **19** 395–408

[69] Watkins C J C H 1989 *Learning from delayed rewards* (King's College, Cambridge United Kingdom)

[70] Mnih V, Kavukcuoglu K, Silver D, Graves A, Antonoglou I, Wierstra D and Riedmiller M 2013 Playing atari with deep reinforcement learning *arXiv preprint arXiv:1312.5602*

[71] Mnih V, Badia A P, Mirza M, Graves A, Lillicrap T, Harley T, Silver D and Kavukcuoglu K 2016 Asynchronous methods for deep reinforcement learning *International conference on machine learning* (PMLR) pp 1928–37

[72] Schaul T, Quan J, Antonoglou I and Silver D 2015 Prioritized experience replay *arXiv preprint arXiv:1511.05952*

[73] McKay M D, Beckman R J and Conover W J 2000 A comparison of three methods for selecting values of input variables in the analysis of output from a computer code *Technometrics* **42** 55–61

[74] Plaat A 2022 *Deep reinforcement learning* vol 10 (Springer)